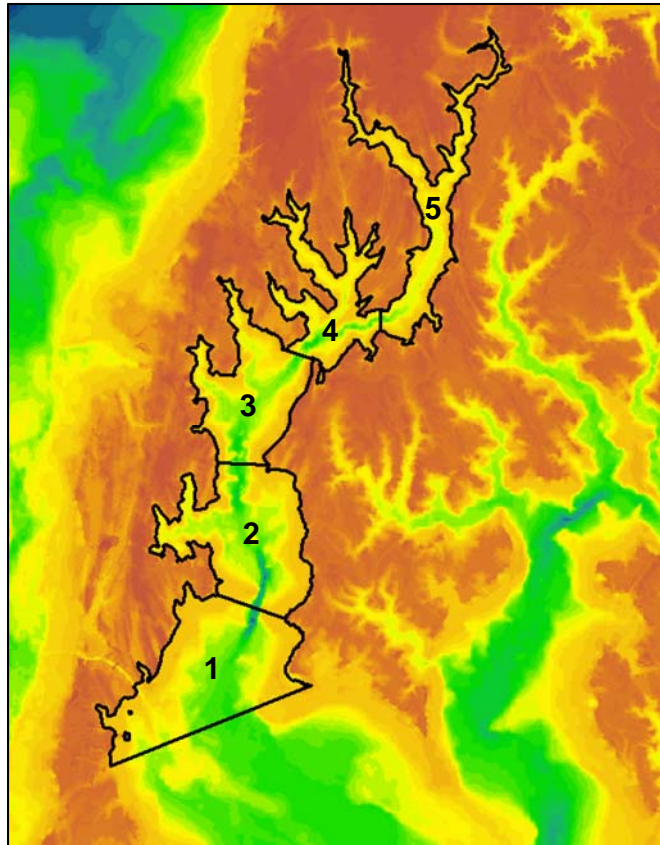


AN UPDATED MODEL FOR ESTIMATING THE TMDL- RELATED BENEFITS OF OYSTER REEF RESTORATION



6/29/2018

Harris Creek, Maryland, USA

A final report to:
The Nature Conservancy
and
Oyster Recovery Partnership

Prepared by:
M. Lisa Kellogg, Mark J. Brush, Jeff C. Cornwell

VIMS | WILLIAM & MARY
VIRGINIA INSTITUTE OF MARINE SCIENCE


University of Maryland
CENTER FOR ENVIRONMENTAL SCIENCE

An updated model for estimating the TMDL-related benefits of oyster reef restoration

HARRIS CREEK, MARYLAND, USA

Award Information

Project Title: An updated model for estimating the TMDL-related benefits of oyster reef restoration in Harris Creek, MD

Principal Investigators:

M. Lisa Kellogg, Virginia Institute of Marine Science

Mark J. Brush, Virginia Institute of Marine Science

Jeff C. Cornwell, University of Maryland Center for Environmental

Award Period: 15-July-2015 to 30-June-2018

Grantee Org.: Virginia Institute of Marine Science

Contact Person: Lisa Kellogg
lkellogg@vims.edu
804-684-7706

Model Information

Web Address: exchange.iseesystems.com/public/markbrush/harris-creek-model-v2

Contact Person: Mark Brush
brush@vims.edu
804-684-7402

Abstract

In 2014, a user-friendly, web-accessible model was developed that allowed restoration practitioners and resource managers to easily estimate the TMDL-related benefits of oyster reef (*Crassostrea virginica*) restoration per unit area, run restoration scenarios in Harris Creek, MD to optimize restoration planning and implementation, and calculate the benefits of the chosen plan. The model was rooted in scientifically defensible data and was readily transferrable to systems throughout the Chesapeake Bay and Eastern Shore. The model operated in five vertically well-mixed boxes along the main axis of the creek. Exchanges among creeks were computed using a tidal prism approach and were compared to exchanges provided from a high resolution 3D hydrodynamic model. Watershed inputs for the model were obtained for the Harris Creek sub-watershed from the Phase V Chesapeake Bay Program Watershed Model. The base model simulated daily concentrations over an annual cycle of chlorophyll-a, dissolved inorganic nitrogen (N) and phosphorus (P), dissolved oxygen, total suspended solids, the biomass of benthic microalgae, and the water column and sediment pools of labile organic carbon (C) and associated N and P. Water quality data for model forcing and calibration were obtained from the Chesapeake Bay Program, the Choptank Riverkeeper, the University of Maryland Center for Environmental Science, and the Maryland Department of Natural Resources. An oyster sub-model was coupled to this base model to compute the volume of water filtered, removal of phytoplankton, suspended solids, and associated nutrients via filtration, recycling of nutrients and consumption of oxygen by oyster respiration, production of feces, N and P accumulation in oyster tissues and shell, oyster-enhanced denitrification, and N and P burial associated with restored reefs. The completed model was served online and operated through a web browser, enabling users to conduct scenario analysis by entering box-specific values for acres restored, restored oyster density, and restored oyster size, as well as the economic value of associated N and P removal.

The updated model incorporates all aspects of the previous model but replaces oyster related data collected outside Harris Creek with site-specific data, and now includes restored oyster populations and water quality data through 2016. It also incorporates the impacts of two common, reef-associated filter feeding organisms: the hooked mussel *Ischadium recurvum* and the sea squirt *Molgula manhattensis*. Additional data collected in Harris Creek and incorporated into the model include: biomass of benthic microalgae, biogeochemical fluxes in relation to oyster biomass, and the biomass density and distribution of the dominant non-oyster reef filter feeders (*I. recurvum*, and *M. manhattensis*). The revised model incorporates an improved estimate of annual oyster growth, uses an improved method for estimating N and P sequestered in tissues and shells, and accounts for the pre-restoration oyster population in Harris Creek. The model also incorporates data on

the filtration capacity of *I. recurvum* and *M. manhattensis* in relation to *C. virginica* collected as part of a previous study (not in Harris Creek) by Kellogg and Newell (unpublished data).

Rationale

Efforts to restore viable oyster reefs and expand oyster populations in Chesapeake Bay and elsewhere have been increasingly motivated by the desire to enhance ecological functions and attendant ecosystem services. Increasingly, interest has focused on the potential use of oyster reef restoration and oyster aquaculture as a means of mitigating the effects of eutrophication (Newell 1988, Newell 2004, Coen et al. 2007, Rose et al. 2014, Kellogg et al. 2014b). The United States Environmental Protection Agency's implementation of a nutrient reduction program for Chesapeake Bay (US EPA 2010) has further heightened interest in the potential water quality benefits of oyster reef restoration. US EPA is using a Total Maximum Daily Load (TMDL) approach toward setting nutrient reduction targets. In January 2017, the EPA provided a legal opinion to the Chesapeake Bay Program Partnership's Oyster BMP Expert Panel stating that restored oyster reefs could be considered by the Panel for approval as a best management practice for removing nitrogen, phosphorus and sediments from Chesapeake Bay waters (USEPA 2018). However, relatively few quantitative tools exist to compute the TMDL- and ecosystem-level benefits of oyster restoration. The model developed as part of this project seeks to partially fill this need by providing a scientifically defensible means of estimating the water quality benefits of oyster reef restoration in Harris Creek, MD. Understanding that oyster reefs are dynamic systems and that oyster biomass per unit area will change over time, the model intentionally relies heavily on user-entered values for area restored, restored oyster density, and mean individual oyster weight, allowing updated estimates of benefits to be calculated easily as new data on oyster biomass become available.

Focusing on the first of a planned series of tributary-scale oyster reef restoration efforts (US ACE 2012), our goal was to use scientifically defensible data to develop a user-friendly, web-accessible model that would allow restoration practitioners and resource managers to easily estimate the TMDL-related benefits of oyster reef restoration per unit area. Model outputs needed to include the: 1) amount of N removed via denitrification, 2) volume of water filtered, 3) amount of chlorophyll-a and suspended solids removed from the water column, 4) amounts of N and P buried in the sediments, and 5) amounts of N and P sequestered in animal tissue and shell. The model also needed to include an option for the user to input nutrient trading credits; if entered, the model would estimate the economic value of each restoration option. By implementing a reduced complexity, reduced spatial resolution model in Harris Creek, the model could readily incorporate new data collected as restored reefs change over time. The reduced complexity approach also enables fast run times (seconds to minutes) on personal computers and enables the model to be served online for direct use by stakeholders through a web browser, eliminating the need for purchase and operation of modeling software or extensive modeling expertise.

Model Approach

Spatial and Temporal Resolution:

Given the desire to have a fast-running, online model that is easy to update with new data, Harris Creek was divided into five vertically well-mixed spatial elements or boxes (Fig. 1). The locations of box boundaries were set according to key geomorphic constrictions within the estuary, to capture the main down-estuary gradients in salinity and water quality, and to contain a number of water quality monitoring

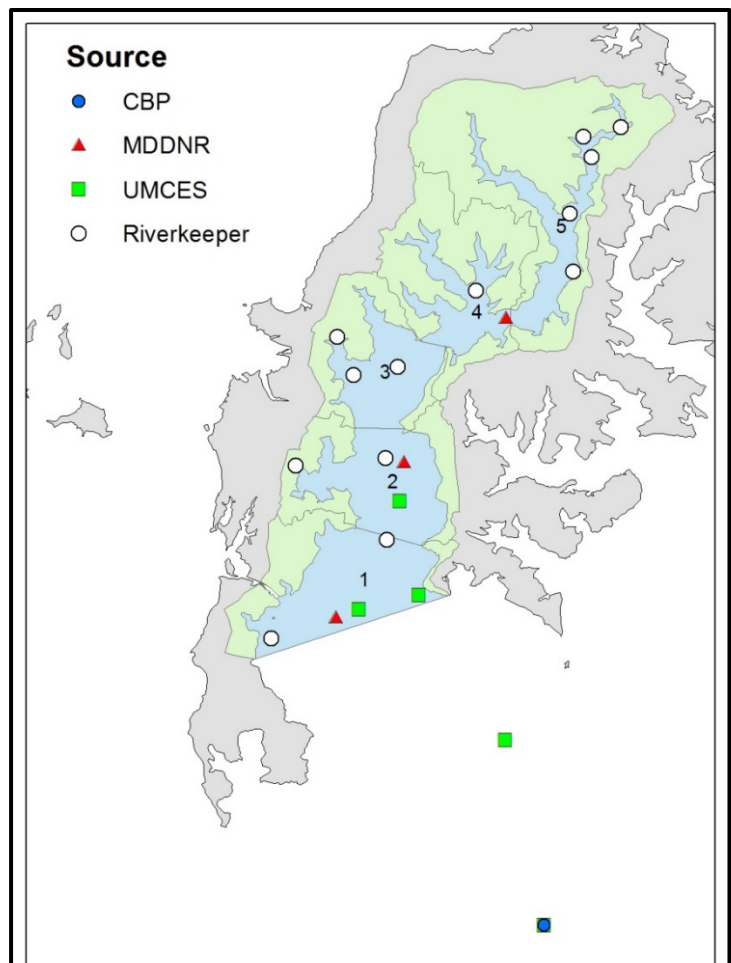


Fig. 1. Model spatial elements, corresponding watersheds (light green polygons), and monitoring stations. Note there is an UMCES station that overlaps with the CBP station (EE2.1). See Table 3 for station details.

stations within each box (as well as outside the system to set boundary conditions).

While a number of monitoring stations exist within Harris Creek (see Fig. 1 and discussion below), the data are somewhat limited in that different stations were sampled in different years (some only for 1-2 years), different parameters were sampled at different stations, and many of the data sets contain data only for the warmer months (e.g., May - October). Given the limited data available for calibration and the desire to have the model capture the long-term mean conditions in the estuary, the model was designed to simulate the average annual cycle of water quality and impacts of restored oyster reefs in the system.

Estuarine Ecosystem Model:

We applied a mechanistic, reduced complexity, management-relevant estuarine ecosystem model that simulates state variables and processes of first-order importance to estuarine eutrophication (Fig. 2; Brush and Nixon 2017). The model simulates daily concentrations over an average annual cycle of chlorophyll-a (Chl), C, N, and P in both phytoplankton (PHYTO) and benthic microalgae (BMA); the water column pools of total suspended solids (TSS), dissolved oxygen (DO or O₂),

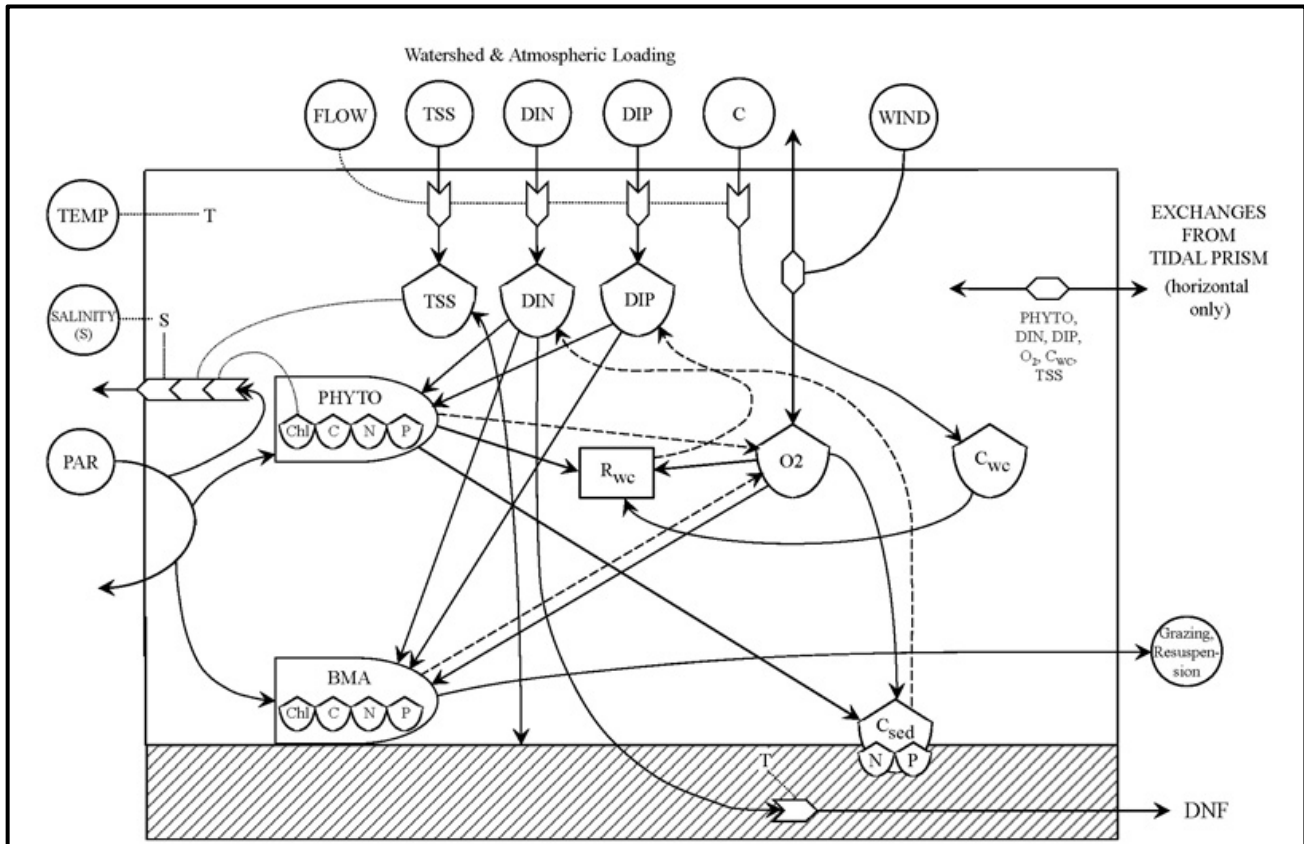


Fig. 2. Schematic of the estuarine ecosystem model applied to Harris Creek. All terms are defined in the text.

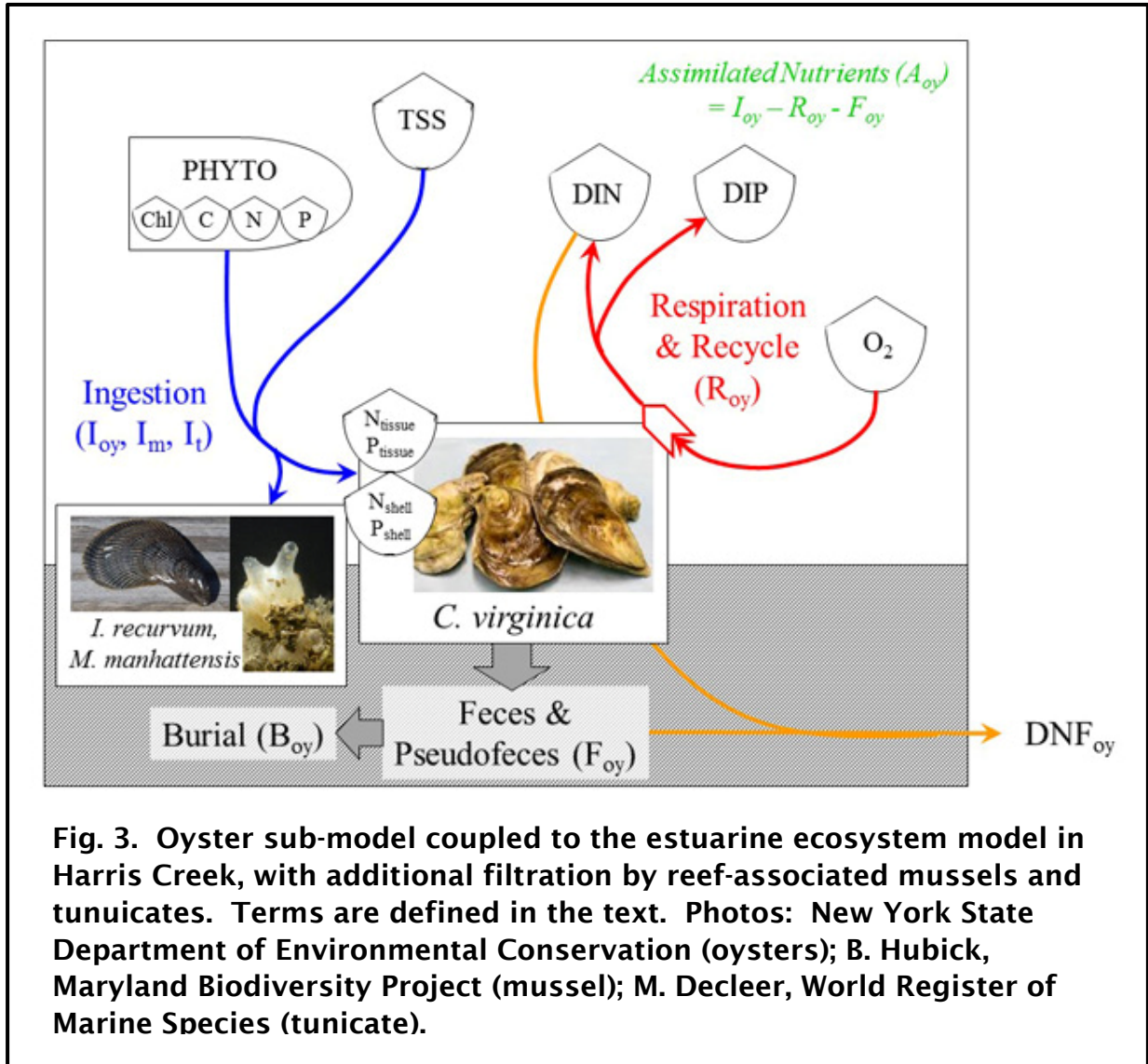
dissolved inorganic nitrogen (DIN), and dissolved inorganic phosphorus (DIP); and the pools of labile organic carbon (C_{wc} and C_{sed}) and associated N and P in the water column and sediments, respectively. The model is forced with daily water temperature (TEMP or T), salinity (S), photosynthetically active radiation (PAR), inputs of freshwater (FLOW), TSS, DIN, DIP, and C from the watershed, atmospheric deposition of N, and mean wind speed. Exchanges between spatial elements and with the lower Choptank River are computed using a tidal prism approach; boundary conditions in the lower Choptank are forced from long-term monitoring data (see below). A core set of key rate processes (phytoplankton production, water column respiration or R_{wc}, carbon flux to the sediments, and denitrification or DNF in the absence of oysters) are formulated using robust, cross-system empirical relationships shown to apply across a wide range of temperate estuaries and rooted in actual measurements, thereby reducing the number of unconstrained parameters and uncertainty in model predictions (Brush et al. 2002; Brush and Nixon 2017). This approach is in line with recent calls for management-relevant models of reduced complexity as an alternative to more complex, highly parameterized models (e.g., NRC 2000; Duarte et al. 2003; Ganju et al. 2015).

While the reduced spatial resolution of the Harris Creek Model enables fast run times through an online platform, it necessarily loses fine-scale spatial and temporal variations in hydrodynamics. In our previous report (Kellogg et al. 2014a), we calibrated our tidal prism exchanges against those produced by the fine-scale 3D Choptank Regional Ocean Modeling System (ChopROMS, North et al. 2012) to ensure the box model was producing the correct magnitude of volume exchange across all five box boundaries.

Oyster Sub-Model:

We coupled a model of restored oyster reefs (Fig. 3) to the estuarine ecosystem model above. The oyster model computes the daily growth of an individual oyster based on the balance between ingestion, production of feces, and respiration. Model formulations are based on Ehrich and Harris (2015), Cerco and Noel (2005, 2007), and Fulford et al. (2007). Briefly, filtration is a function of individual weight, water temperature, salinity, TSS, and DO. Individual filtration is multiplied by total oyster abundance and used to draw down the pools of TSS, phytoplankton biomass, and associated N and P which are allocated to tissue and shell (N_{shell}, N_{tissue}, P_{shell}, P_{tissue}, see below). Ingested material is converted to assimilated material using an assimilation efficiency; the balance is deposited as feces. Respiration is a combined function of a temperature-dependent basal rate and a constant fraction of daily assimilation, and is used to consume O₂ and recycle DIN and DIP back to the water column. Oyster-enhanced rates of denitrification (DNF_{oy}) are computed using an empirical regression based on direct measurements in

Harris Creek (see below). A constant fraction of N and P deposited in feces is buried (see below). The revised model now also includes filtration of phytoplankton and TSS by *I. recurvum* and *M. manhattensis* associated with the restored oyster reefs (see below).



Data Sources and Assumptions

The following sections refer to a number of figures showing model forcing data and calibration results. These figures have been compiled at the end of this report in Appendix A.

Estuarine Ecosystem Model:

Delineation of Harris Creek box boundaries and associated watersheds was conducted in ArcGIS. The coastline was obtained from the Chesapeake Bay Program and edited to divide the system into five boxes. Watersheds for each box were delineated manually using the National Hydrography Dataset (NHD, nhd.usgs.gov) high resolution stream lines and National Elevation Dataset (NED, ned.usgs.gov) 2013 1/3 arc-second grid. Mean depths of each box were re-computed using the new 2016 USGS seamless topobathic surface for the Chesapeake Bay watershed (USGS 2016). The mean tide range (0.41 m, mean high water – mean low water) for computation of tidal prism exchanges was taken as the average of the current tidal datums at the Cambridge (0.49 m) and Poplar Island (0.34 m) NOAA tide stations. Resulting areas, depths, and volumes used in the Harris Creek Model are shown in Table 1. To enable more accurate simulation of benthic microalgal biomass and nutrient cycling, box bottom area was divided into the area within 0.5 m depth increments down to 2 m (Table 2).

Table 1. Dimensions of the Harris Creek Model spatial elements. Depths are relative to mean sea level.

Box	Watershed Area, m ²	Open Water Area, m ²	Mean Depth, m	Volume, m ³	Tidal Prism Volume, m ³
1	2,533,048	5,244,487	2.35	12,315,239	2,150,240
2	2,740,880	4,330,030	2.29	9,909,786	1,775,312
3	2,653,766	3,156,203	2.15	6,789,785	1,294,043
4	5,647,320	2,329,933	1.65	3,850,873	955,273
5	11,091,800	2,658,286	1.38	3,680,169	1,089,897

Watershed loads into each spatial element were determined using output for 1985-2005 for the Harris Creek polygon of the CBP Phase V Watershed Model. Monthly loads across all years of freshwater, DIN, DIP, TSS, and organic C were used to compute mean monthly values (Fig. A1). Monthly loads of freshwater to the entire creek were forced directly into the model, converted to a yield of freshwater (per unit area of watershed), and multiplied by the area of each box watershed to compute the input to each box. Material loads (i.e., DIN, DIP, TSS, organic C) were converted to mean concentrations in the inflowing water which were forced into

Table 2. Open water area (m²) by depth segment for the benthic microalgal submodel. Depths are relative to mean sea level.

Depth Segment, m	Box 1	Box 2	Box 3	Box 4	Box 5
0 - 0.5	318,067	238,901	199,788	201,848	352,679
0.5 - 1	1,215,099	949,950	617,933	519,158	623,548
1 - 1.5	419,387	503,092	389,021	446,245	575,058
1.5 - 2	509,981	358,936	365,185	419,122	500,135
> 2	2,781,953	2,279,151	1,584,276	743,560	606,866

the model and used to compute the load to each box. An average daily value for atmospheric N deposition onto each box of $0.53 \text{ g N m}^{-2} \text{ y}^{-1}$ was computed using annual wet and dry deposition data for 2011 to 2016 from the National Atmospheric Deposition Program station at Wye, MD (MD13) and the EPA Clean Air Status and Trends Network station at the Blackwater National Wildlife Refuge (BWR139), respectively. This is revised down from the older, Chesapeake Bay mean value of $1 \text{ g N m}^{-2} \text{ y}^{-1}$ used in the original Harris Creek Model from Boynton et al. (1995). Deposition of P was assumed to be negligible.

Water quality data from four sources were updated through 2016 for use in revised model forcing and calibration (Table 3, Fig. 1). The CBP has conducted approximately monthly sampling since 1984 of a variety of parameters at station EE2.1 in the lower Choptank River outside the mouth of Harris Creek. The Maryland Department of Natural Resources (MDDNR) operates three high frequency water quality data sondes in the creek. The upper and lower sondes are moored at depths of approximately 3 m; the middle station is a vertical profiler in about 3 m of water from which readings at 1 m were extracted. Values at all depths were used to confirm that stratification is minimal at the site (Fig. A2). MDDNR also collects regular water quality samples at each site during calibration cruises. The monitoring data from the University of Maryland Center for Environmental Science (UMCES) were derived from the TRANSPORT Program and were collected from May through September in 2010, 2011, and 2012 at stations in the lower creek and Choptank River (North unpublished data). Finally, Mr. Drew Koslow and Mr. Tim Rosen (Choptank Riverkeeper, Midshore Riverkeeper Conservancy) provided approximately monthly citizen science monitoring data from several stations throughout Harris Creek.

Table 3. Updated sources of data used to develop and calibrate the Harris Creek Model. The last column indicates the corresponding spatial element for each station, or if the station was used to set the boundary conditions. See text for abbreviations.

Source	Parameters	Station	Years ^a	Box
CBP	T, S, DO, TSS, Chl-a, DIN, DIP	EE2.1	2000-16	Boundary
MDDNR ^b	T, S, DO, Chl-a	XFG2810 (Conmon)	9/13-12/16	1
		XFG4618 (Profiler)	6/12-12/16	2
		XFG6431 (Conmon)	9/13-12/16	4
	Chl-a, TSS, DIN, Secchi depth, k_D	XFG2810 (Discrete)	9/13-12/16	1
		XFG4618 (Discrete)	6/12-12/16	2
		XFG6431 (Discrete)	9/13-12/16	4
UMCES	T, S, DO, TSS, Chl-a	2	2010-12	Boundary
		3	2010-12	Boundary
		21	2010-12	1
		22	2010-12	1
		20	2010-12	2
Riverkeeper	T, S, DO, Chl-a, Secchi depth	HC06	2012-16	1
		HC09	2010-11	1
		HC05	2012-16	2
		HC08	2010-11	2
		HC04	2010-16	3
		HC07	2010-11	3
		HC03	2012-16	4
		HC01	2010-16	5
		HC02	2012-16	5
HC14	2010-13	5		

^a Data from sources other than the CBP are primarily from warmer months only.

^b MDDNR data are from two continuous monitoring (Conmon) datasondes and one vertical profiler, with discrete samples collected from calibration cruises at the same locations.

Oyster Sub-Model:

Area of restored reefs in each box was computed from the April 3, 2017 version of the Harris Creek Oyster Restoration Blueprint Geodatabase provided by the NOAA Chesapeake Bay Office. Values represent all restoration activities through 2016 and include both ‘alternate substrate & seed’ and ‘seed only’ sites. Mean live oyster densities and mean individual oyster mass (g dry weight, DW) were based on the most recent available survey data (NOAA 2016, NOAA 2017; Table 4). Because data were not available for all reefs and because data suggested differences in density between the two restoration types, mean oyster density and mass within each box were first computed for both restoration types and then weighted by relative area of each type. These values are provided as defaults in the online Harris Creek Model. Accuracy of the estimated TMDL-related benefits of oyster reef restoration in Harris Creek will depend heavily upon the accuracy of the values entered by the user. Default values can be changed as additional data become available from restored reefs in Harris Creek.

Table 4. Area of restored reefs, mean live oyster density, and mean individual oyster mass used as defaults in the model. The estimated total post-restoration population is 1.34×10^8 oysters.

Box	Acres Restored	Mean Live Density, # m ⁻²	Mean Individual Mass, g DW
1	168.6	118.0	0.95
2	88.5	55.5	0.87
3	65.6	70.2	1.08
4	17.9	172.0	1.28
5	6.9	91.5	1.26

Reef polygons from the Blueprint Geodatabase were merged with the USGS (2016) seamless topobathic surface to estimate mean water column depth over the reefs in each box, and thus water column volume overlying the reefs, and the fraction of total area and volume in each box composed of reefs (Table 5). Mean distance to reefs within each box from the mouth of Harris Creek was required for some of the empirical regressions (see below), and was computed in ArcGIS using the centroid of each reef polygon (Table 5).

Current estimates of the oyster population in Harris Creek derived from the Blueprint Geodatabase (i.e., Table 4) are based on recent surveys and include oysters that were present prior to restoration. To assess the impact of only restored oysters, the pre-restoration oyster population was estimated using the survey data from Versar (2012) conducted in early 2012, excluding the Mill Point

Table 5. Mean reef depth relative to mean sea level in each box, reef area and water volume overlying reefs in each box, and mean distance of reefs in each box from the mouth of Harris Creek.

Box	Mean Reef Depth, m	Reef Area, m ²	Overlying Volume, m ³	Mean Distance, km
1	2.81	693,040	1,944,411	0.69
2	2.97	379,435	1,126,473	3.46
3	2.72	273,146	744,166	5.54
4	3.38	74,857	252,695	7.25
5	2.56	29,341	74,990	8.61

and Turkey Neck sites which were restored in 2011. Versar (2012) provided estimates of live oyster density and total number of oysters on each reef, which were used to compute reef area and mean density within each box (Table 6). Versar (2012) also estimated the number of oysters in three size categories (market, small, and spat), which allowed calculation of the percent of the population in each category. Versar’s (2012) reported shell height range for each size class was converted to dry weight using a height-weight regression for Harris Creek (see below), and these were in turn used to assign average weights to each size class (1.29, 0.24, and 0.01 g DW, respectively). Mean individual mass of pre-restored oysters in each box was then computed using these weights and the percent of the population in each size class (Table 6).

Table 6. Estimated area of reefs, mean live oyster density, and mean individual oyster mass of the pre-restored oyster population in Harris Creek. The estimated total pre-restoration population is 4.54×10^6 oysters.

Box	Acres	Mean Live Density, # m ⁻²	Mean Individual Mass, g DW
1	189.5	3.0	0.31
2	55.0	2.2	0.38
3	114.6	1.1	0.40
4	89.6	3.2	0.42
5	53.5	0.2	0.77

In 2015, data on oysters, macrofauna, and biogeochemical fluxes were collected seasonally in Harris Creek as part of multiple projects supported by other funding sources (Cornwell et al. 2016, Kellogg et al. 2016). Wherever appropriate, these data were used to update model functions. However, data were only collected from oyster reefs restored using juvenile oysters set on shell and planted directly on the substratum without the addition of a shell or rock base. If restoration sites that utilize a shell or rock base differ significantly from those which do not use a rock or shell base, the updated model may significantly underestimate or overestimate the ecosystem services provided by oyster reef restoration in Harris Creek.

The conversions between tissue dry weight and shell height and weight were determined using all measurements collected in Harris Creek (Fig. 4). These relationships are used whenever necessary in the model; the relationship between tissue and shell mass is particularly used for computing shell mass from modeled individual weight, which are both used to compute the amount of nitrogen and phosphorus sequestered in oyster tissue and shell. The latter calculation is based upon mean values for the percentage of N and P in oyster tissue and shell from the Choptank River (Table 7, Kellogg et al. 2013).

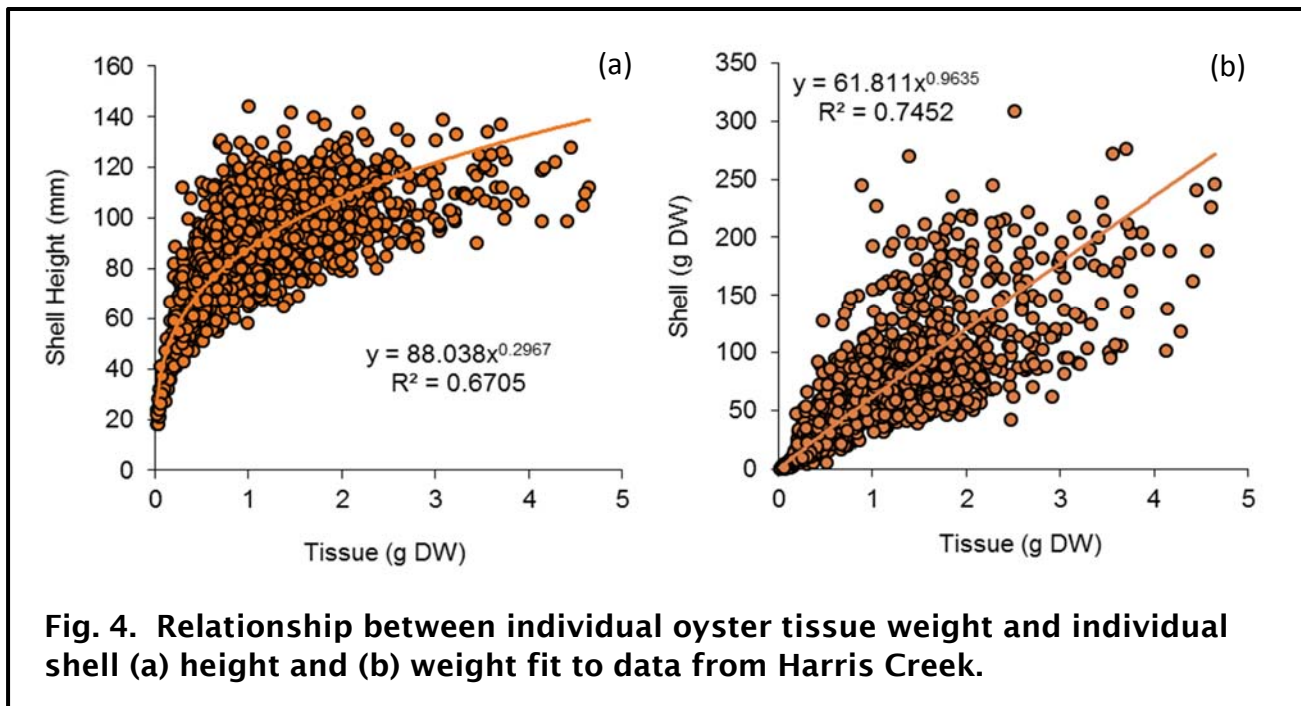


Fig. 4. Relationship between individual oyster tissue weight and individual shell (a) height and (b) weight fit to data from Harris Creek.

Table 7. Mean nitrogen and phosphorus content of oyster tissue and shell, expressed as a percent of dry weight, using data from Kellogg et al. (2013).

Box	%N	%P
Tissue	9.27	1.26
Shell	0.21	0.04

The ash free dry weight (AFDW) biomass density of mussels (g AFDW m^{-2}) is modeled as a function of total oyster biomass density (g DW m^{-2}):

$$\text{Ischadium AFDW} = 0.1176 * \text{Total Oyster DW}$$

This regression was fit to observed data from Harris Creek and reproduces the observations (Fig 5a). AFDW is then converted to dry weight based on the regression in Fig. 5b.

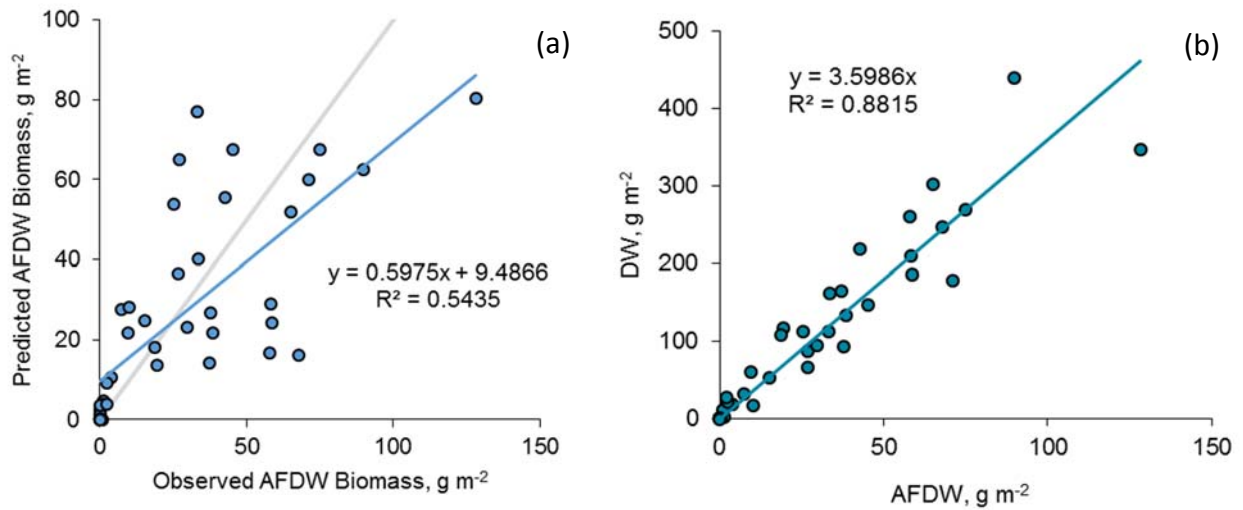


Fig. 5. (a) Relationship between observed and predicted mussel biomass density based on the empirically fit linear regression. Blue line is the regression between observed and predicted values; grey line denotes the 1:1 relationship. (b) Conversion between mussel tissue AFDW and DW.

The biomass density of tunicates (g AFDW m⁻²) is modeled as a function of water temperature (°C) and distance from the mouth of the creek (km), constrained to not go below zero:

$$\text{Mogula AFDW} = 57.5 - (5 * \text{Distance}) - (1.5 * \text{Temperature})$$

This multiple regression was fit to observed data from Harris Creek and reproduces the observations (Fig 6a). AFDW is then converted to dry weight based on the regression in Fig. 6b.

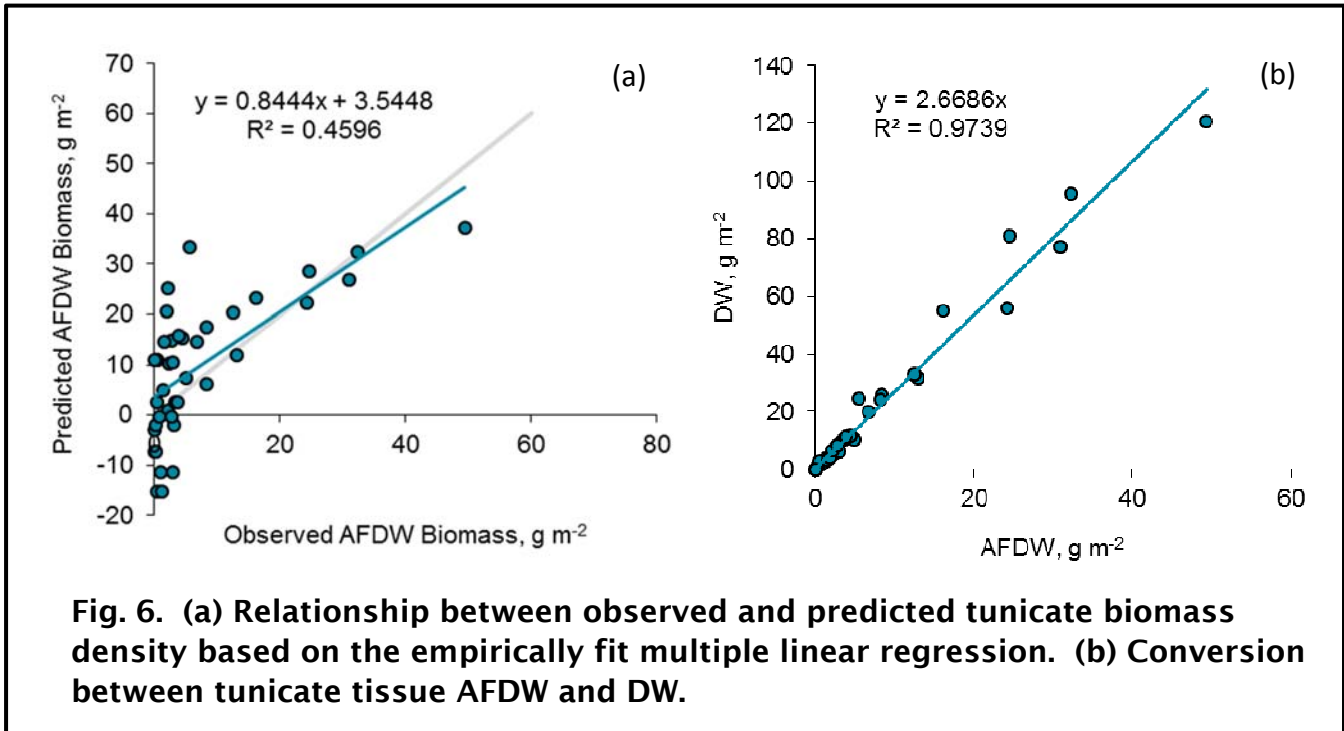


Fig. 6. (a) Relationship between observed and predicted tunicate biomass density based on the empirically fit multiple linear regression. (b) Conversion between tunicate tissue AFDW and DW.

As described above, filtration capacity of oysters is a function of individual weight, water temperature, salinity, TSS, and DO. The filtration capacity of mussels and tunicates is scaled to that of oysters based on the results of previous laboratory studies (Fig. 7, Kellogg and Newell, unpublished data). While this approach works well for months when oysters are actively filtering, we recognize that it likely underestimates the annual filtration capacity of tunicates which are capable of filtering at lower water temperatures than oysters. As for oysters, filtration rates of mussels and tunicates are used to compute ingestion of phytoplankton, TSS, and associated nitrogen and phosphorus. While computed removal of chl-a and TSS by these groups can be readily compared to that removed via oyster filtration, the model does not compute recycling or biodeposition of nutrients ingested by mussels and tunicates, so nutrient removals computed for these groups should be

taken as an upper estimate. However, nitrogen that is denitrified from mussel and tunicate biodeposits should be inherently included in modeled reef denitrification, which is based on observed rates reflective of the entire reef community.

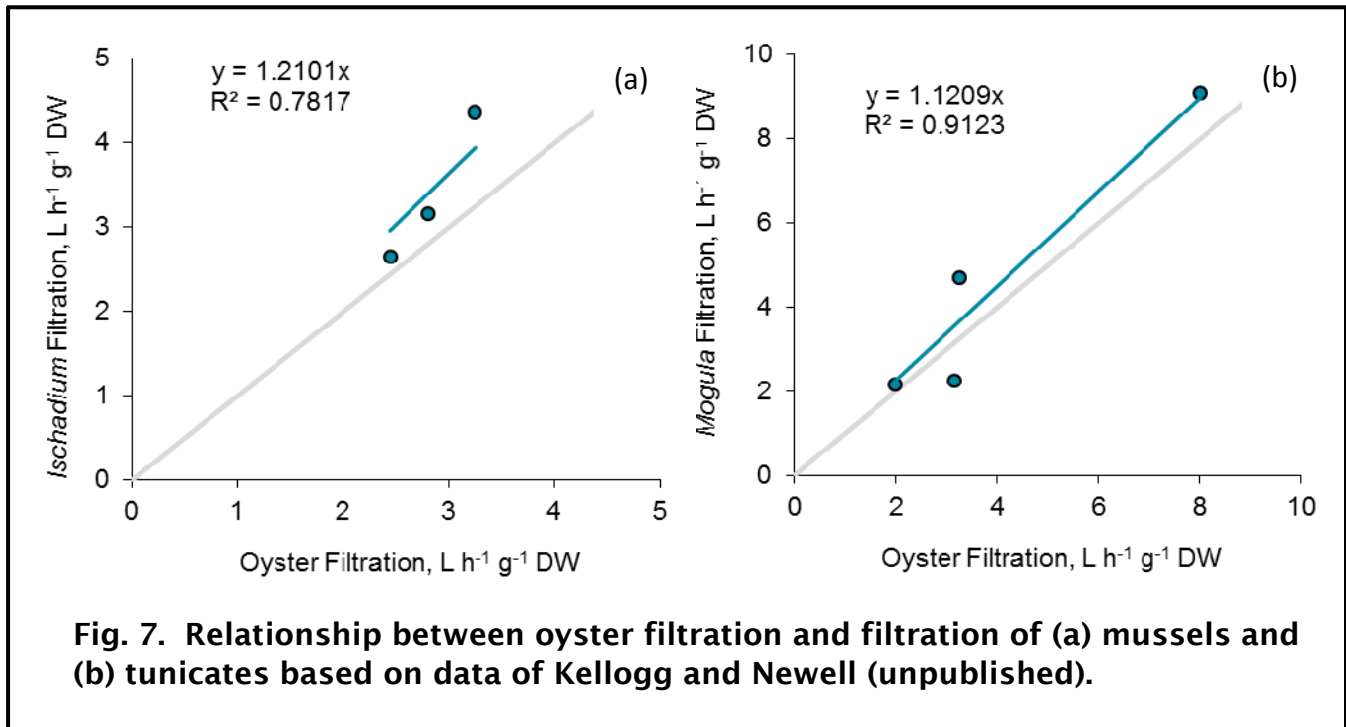


Fig. 7. Relationship between oyster filtration and filtration of (a) mussels and (b) tunicates based on data of Kellogg and Newell (unpublished).

Oyster-enhanced denitrification ($\mu\text{mol N}_2\text{-N m}^{-2} \text{h}^{-1}$) was best modeled as a function of the biomass density (g AFDW m^{-2}) of the polychaete worm *Alitta succinea*:

$$\text{N}_2 \text{ Flux} = 54.08 * \text{Alitta AFDW}$$

This regression was fit to pooled observations conducted in the light and dark from Harris Creek and reproduced the observations (Fig. 8). Because the denitrification function is based entirely on measurements from reefs restored using oysters and oyster shell, model estimates may significantly over- or underestimate actual values if denitrification rates on reefs restored using a shell or stone base differ significantly from those using only spat settled on oyster shell.

The ash free dry weight (AFDW) biomass density of *Alitta succinea* (g AFDW m^{-2}) is in turn modeled as a saturating function of mussel biomass density (g AFDW m^{-2}) and an exponential function of water temperature:

$$\text{Alitta AFDW} = 11.951 * (1 - e^{(-0.039 * \text{Ischadium})}) * e^{[-0.016 * (\text{Temperature} - 20.977)^2]}$$

This nonlinear regression was fit to observed data from Harris Creek and reproduces the observations (Fig 9a). AFDW is then converted to dry weight based on the regression in Fig. 9b.

As in the previous version of the model, no direct estimates exist for burial of N and P from biodeposits, so we used the rate of 10% from Newell et al. (2005).

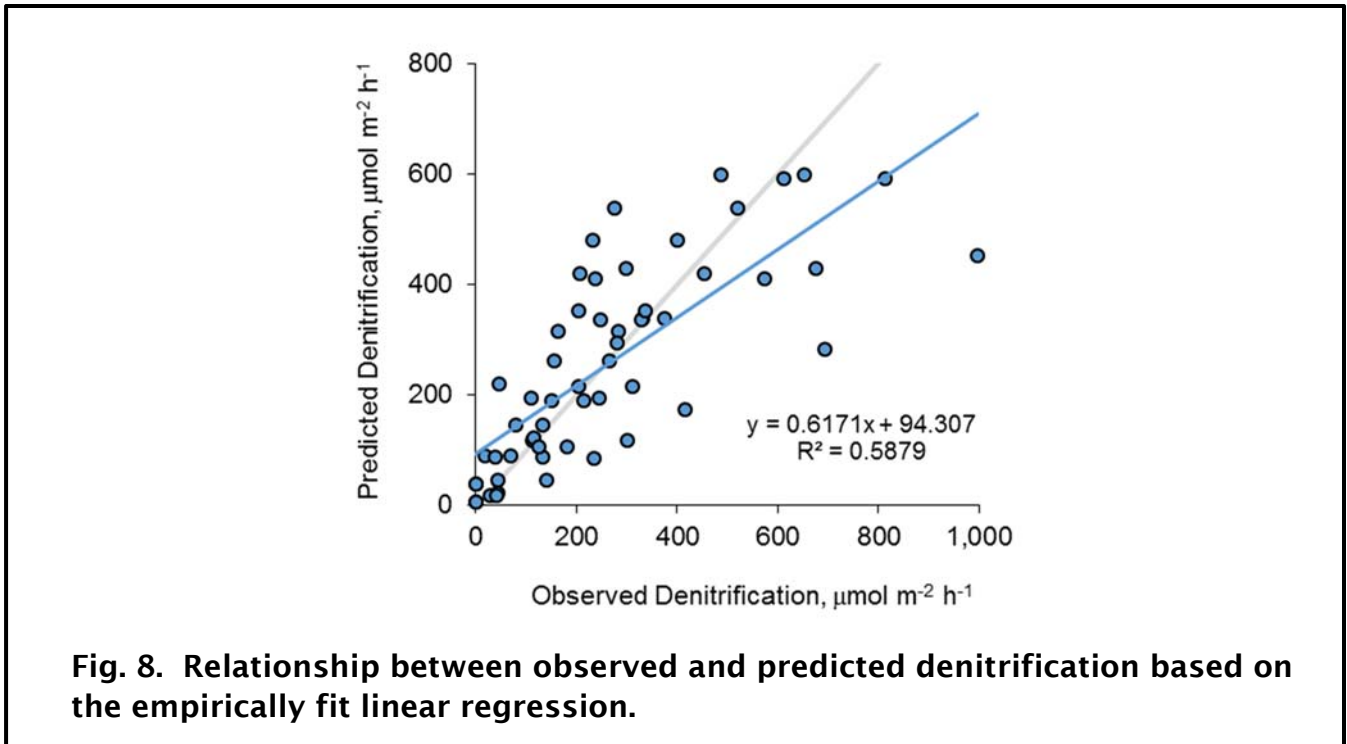


Fig. 8. Relationship between observed and predicted denitrification based on the empirically fit linear regression.

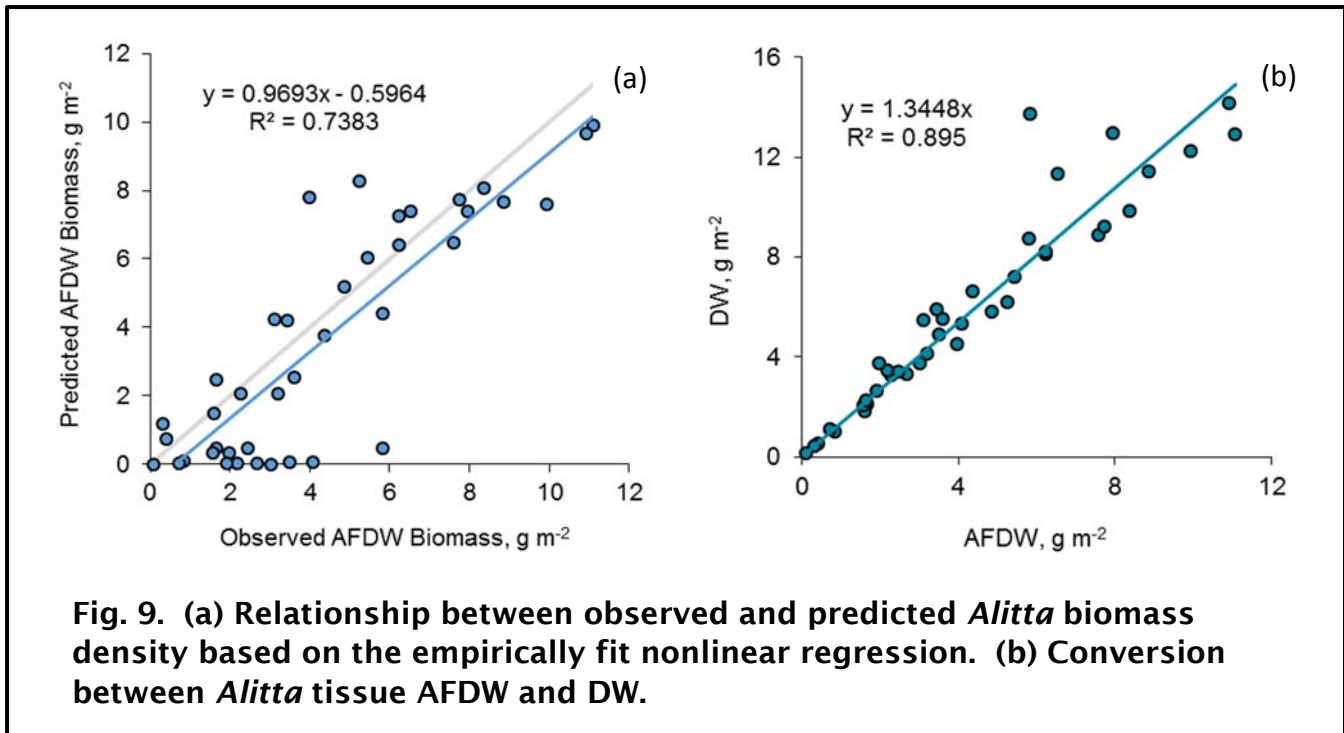


Fig. 9. (a) Relationship between observed and predicted *Alitta* biomass density based on the empirically fit nonlinear regression. (b) Conversion between *Alitta* tissue AFDW and DW.

Model Implementation, Calibration, and Predictions

Forcing Functions:

CBP data at station EE2.1 in the lower Choptank River were interpolated to daily resolution and used to compute mean annual cycles of each parameter to force at the mouth of Harris Creek (Figs. A3, A4). Interpolated data were used only from 2000 to 2016 to avoid earlier changes in detection limits and an increasing trend in chl-a prior to 2000. UMCES data at the two stations outside the creek fell mostly within the interannual variability (i.e., ± 2 SD) around the CBP mean annual cycles; therefore, the CBP cycles were forced into the model to set the boundary conditions. Regression of surface chl-a and particulate carbon data from station EE2.1 across the entire time series was used to estimate a C:chl-a ratio of 69 g g⁻¹. Data from the MDDNR calibration cruises were used to develop a regression between model-predicted vertical light attenuation coefficient, k_D (m⁻¹), and secchi depth (m):

$$\text{Secchi depth} = 1.27 * k_D^{-1.11} \quad (r^2 = 0.71)$$

Since the focus of the model was on simulating mean annual cycles, we developed smooth cosine functions for water temperature and salinity in each box rather than

forcing actual measurements (Figs. A5, A6). Functions were fit to pass through the majority of the available measurements; however, given the interannual variability in the Chesapeake, especially for salinity, these functions do not capture the relatively fresher conditions that can exist in some years (Fig. A6).

Cosine functions for PAR and photoperiod (fraction of the day that is light) in the Chesapeake region were obtained from Wetzel and Neckles (1986).

Calibration:

As reported previously (Kellogg et al. 2014a), modeled exchanges of water across each box face computed using the tidal prism and 3D ChopROMS approaches matched well (Fig. A7). While the simplified tidal prism approach misses the high frequency variation in ROMS exchanges, it captures the long-term mean exchanges which is sufficient given the reduced spatial resolution of the Harris Creek Model and focus on simulating mean annual cycles.

Relative to the original model application (Kellogg et al. 2014), we now have a substantially expanded dataset for calibration of water quality, including chlorophyll-a (Fig. A8), TSS (Fig. A9), and DO (Fig. A10), due to addition of data through 2016 and the MDDNR calibration cruise dataset. The latter data also made it possible to assess the model calibration for secchi depth (Fig. A11), DIN (Fig. A12), and DIP (Fig. A13). Finally, as part of the current project, we sampled BMA biomass as chl-a in the top 3 mm of sediment during five surveys (Feb, Apr, Jun, Aug, Oct) in 2016. Randomized shore-based stations were generated in model boxes 2, 3, and 4 for each survey, and a single station in each box was sampled in duplicate for benthic chl-a and phaeophytin at 0.25, 0.75, 1.25, 1.75, 2.25, and 2.75 m relative to mean sea level (Fig A14). These depths correspond to the mid-point of the depth layers used in the model to simulate BMA biomass. Samples were extracted in 90% acetone, analyzed on a scanning spectrophotometer before and after acidification, and resulting absorbances were used to compute chlorophyll-a and phaeophytin concentrations using the equations of Lorenzen (1967).

Modeled water quality and BMA biomass generally fell within the range of the monitoring data. Given the boxed approach of the model, output represents a box-wide average, while observations are from individual stations. Modeled chl-a (Fig. A8) is generally near the upper end of the observations, and the seasonal pattern – particularly the spring bloom – is strongly driven by the boundary condition imposed from CBP station EE2.1 (Fig. A3). Modeled TSS closely matches the data from the Riverkeeper, but falls below the data from UMCES (Fig. A9). The latter data were from a limited time period (2011-12) and did not correspond well to the long-term mean concentrations imposed at the boundary from CBP station EE2.1 (Fig. A3), so it was more important to match the Riverkeeper data for this parameter. Modeled DO closely matches the observations from all data sources in

boxes 1, 2, and 4, particularly from the high frequency MDDNR datasondes and vertical profiler (Fig. A10). Data are only available from the Riverkeeper in boxes 3 and 5, and the model captures the upper end of the observations but not the mean.

Modeled secchi depth is generally within the range of the observations, although the model does not capture the higher secchi depths early and late in the year apparent in some boxes (Fig. A11). Based on the limited data available, the model captures the expected annual cycles and approximate values of DIN (Fig. A12) and DIP (Fig. A13). Modeled DIN is particularly good in box 1, although appears high in box 4, while modeled DIP is at the lower end of the observations. Modeled BMA chl-a biomass closely matched the 2016 observations collected as part of this project, when analyzed by depth bin, box and month (Fig. A15).

Limited data were available to assess simulated individual oyster growth. We used a dataset from the Bolingbroke Sand and Black Buoy Reserves in the Choptank River, two sites of high habitat quality, in which shell heights were measured for oysters of known age (Kellogg and Paynter, unpublished data). These data resulted in a tightly constrained relationship between height (mm) and age (y):

$$\text{Age} = 0.1452e^{0.0336 * H} \quad (R^2 = 0.9842)$$

Default starting oyster weights (Table 4) were converted to heights using the conversion in Fig. 4a, which were then used to estimate age with the regression above. We then computed predicted age one year later, and converted that back to height and mass to produce an estimate of projected annual growth for comparison to model output.

Additionally, Liddel (2008) used a series of oyster growth time series in the Chesapeake to develop seasonally fluctuating von Bertalanffy growth functions in which the growth constant (K , y^{-1}) was allowed to vary as a function of water temperature (T) and salinity (S):

$$K = -0.43427 + (0.02539 * T) + (0.01762 * S) + ((T - 17.72692) * ((S - 9.40128) * 0.00312))$$

Liddel (2008) used this constant in the von Bertalanffy growth equation to compute the predicted change in shell height ($H_2 - H_1$, mm) over two successive time points (t_1 and t_2):

$$H_2 - H_1 = (250 - H_1) * (1 - e^{-K * (t_2 - t_1)})$$

This equation was found to predict maximum annual growth trajectories, while a version that accounted for the effects of parasitism on reduced growth often resulted in more realistic trajectories; in the latter version the von Bertalanffy function was reduced by 80% when salinity exceeded 16, by 60% for salinities

between 12 and 16, and by 0% for salinities under 12 (Liddel 2008). We used these functions (with and without disease effects) to compute predicted annual growth under forced conditions of temperature and salinity, to produce a second set of values to compare to model predictions. Growth was computed as both annual changes in shell height and tissue weight using the conversion in Fig. 4a.

The model was calibrated to reproduce growth rates from the Choptank River dataset, by limiting the volume of each box that oysters are able to graze in, a necessary correction since oysters do not have direct access to the entire volume of each box. This was accomplished by multiplying computed filtration rate by the “p-value”, or the proportion of the box in which oysters can feed. Calibrated p-values in boxes 1-3 were remarkably similar to the computed fraction of box area and overlying volume taken up by reefs (Table 8). Values were also quite close in box 4, but diverged in box 5.

Resulting modeled growth rates in terms of both tissue weight and shell height closely matched those predicted from the Choptank River dataset (Figs. 10-11, Tables 9-10). Rates were also quite close to the values predicted by the Liddel (2008) von Bertalanffy approach with disease effects included, particularly in the lower estuary, although values diverged towards the head of Harris Creek. The Liddel maximum model overestimated growth rates.

The combined result of these analyses indicates that the model is able to reproduce the mean annual cycling of key water quality variables and oyster growth within the range of available data. This confirms that the model is sufficient for use as a tool to assess the TMDL-related impacts of oyster restoration scenarios within Harris Creek.

Table 8. Fraction of total box area taken up by oyster reefs, fraction of box volume overlying the reefs, and calibrated model p-value. First two columns are computed from the data in Tables 4 and 5.

Box	Fraction of Area	Fraction of Volume	p-value
1	0.13	0.16	0.133
2	0.09	0.11	0.111
3	0.09	0.11	0.123
4	0.03	0.07	0.129
5	0.01	0.02	0.095

Table 9. Annual increase in individual oyster tissue mass (g DW y⁻¹) predicted by the model and three additional approaches (see text for details).

Method	Box 1	Box 2	Box 3	Box 4	Box 5
Model	0.40	0.40	0.39	0.37	0.38
Choptank River	0.40	0.40	0.39	0.37	0.37
Liddel (2008) reduced	0.29	0.28	0.59	0.45	0.77
Liddel (2008) maximum	0.86	0.83	0.87	1.02	0.85

Table 10. Annual increase in individual oyster shell height (mm y⁻¹) predicted by the model and three additional approaches (see text for details).

Method	Box 1	Box 2	Box 3	Box 4	Box 5
Model	9.6	10.0	8.7	7.5	7.6
Choptank River	9.5	10.1	8.6	7.5	7.6
Liddel (2008) reduced	7.2	7.3	12.4	8.9	14.4
Liddel (2008) maximum	18.3	18.6	17.2	18.0	15.5

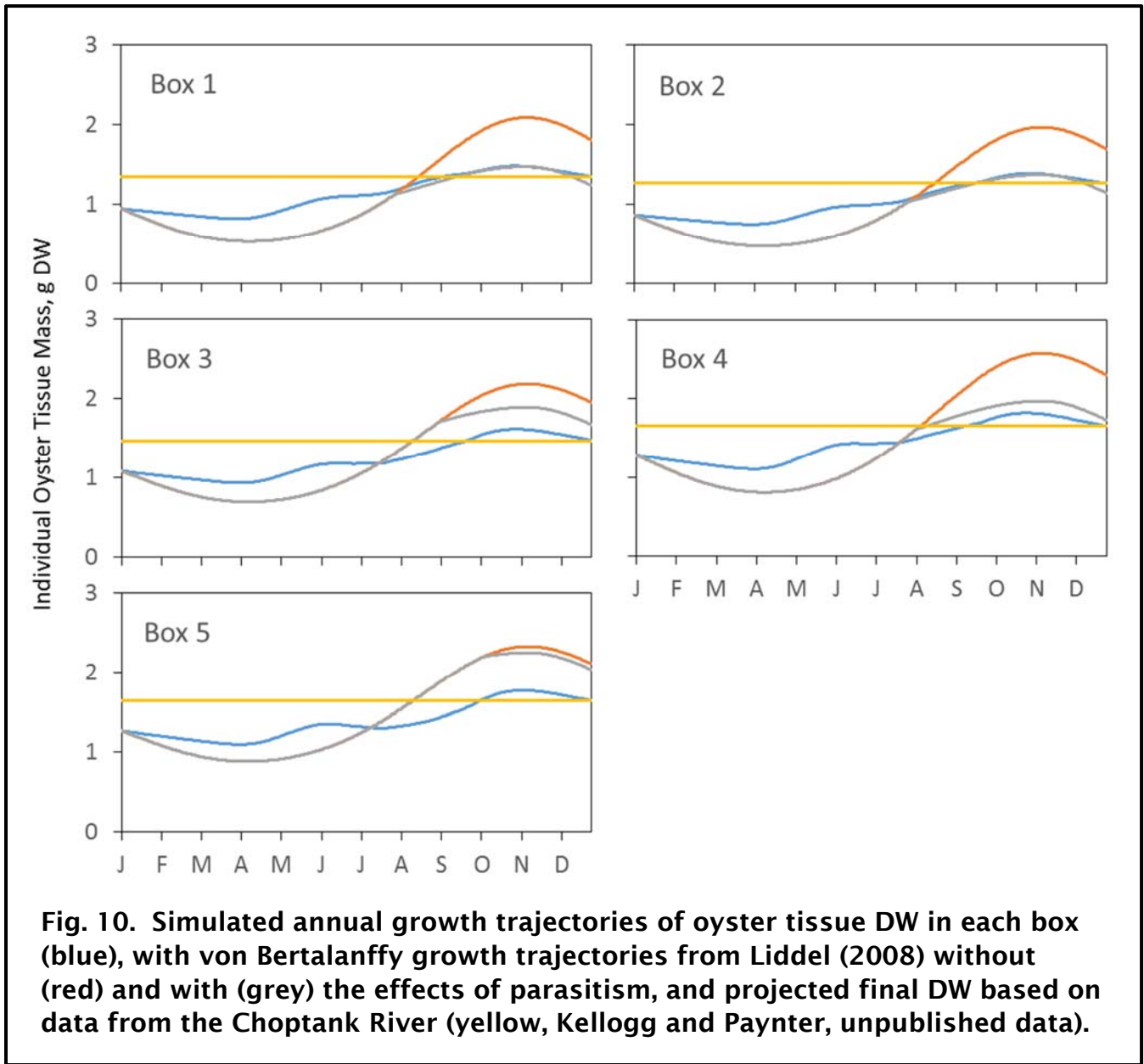


Fig. 10. Simulated annual growth trajectories of oyster tissue DW in each box (blue), with von Bertalanffy growth trajectories from Liddel (2008) without (red) and with (grey) the effects of parasitism, and projected final DW based on data from the Choptank River (yellow, Kellogg and Paynter, unpublished data).

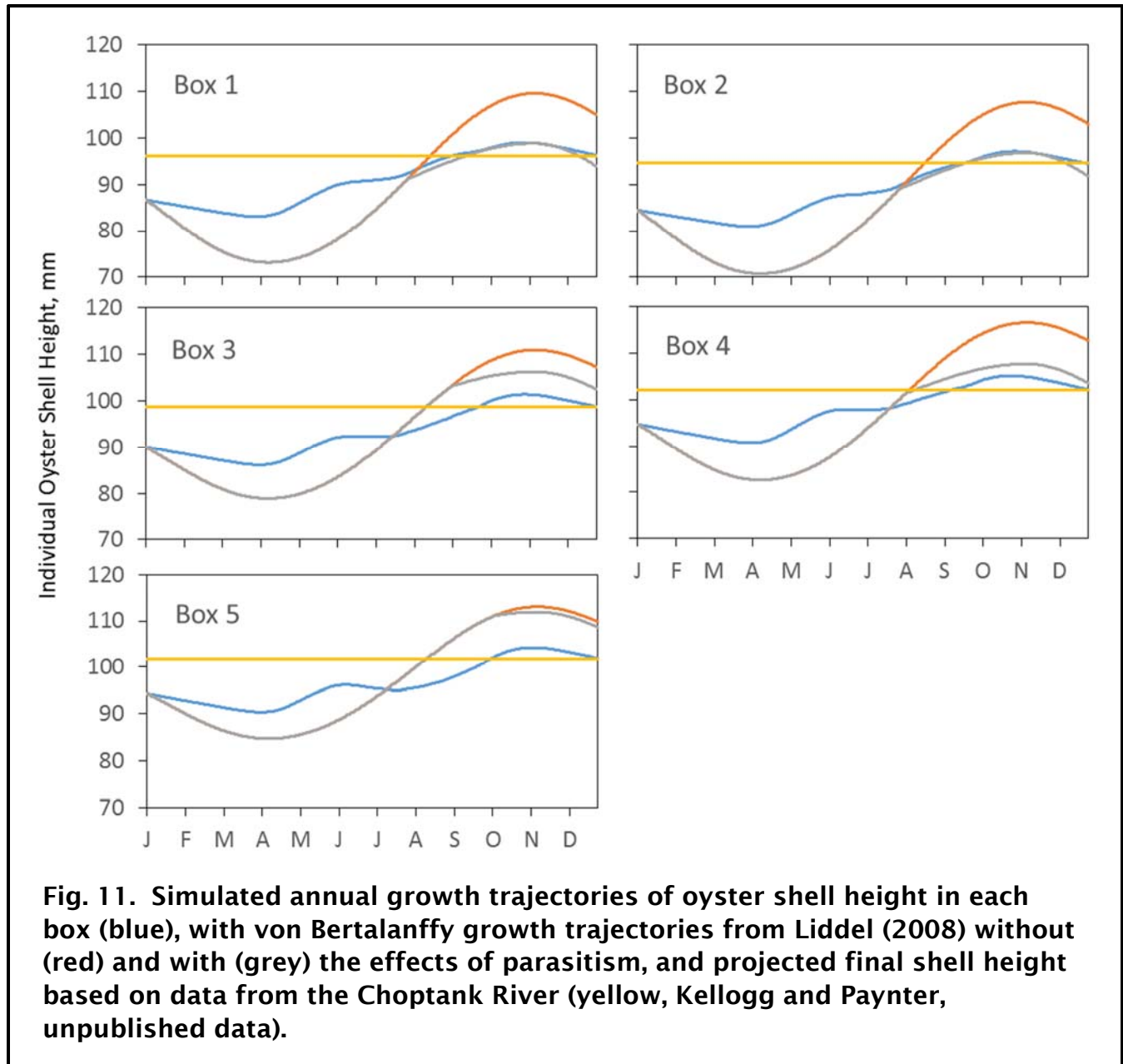


Fig. 11. Simulated annual growth trajectories of oyster shell height in each box (blue), with von Bertalanffy growth trajectories from Liddel (2008) without (red) and with (grey) the effects of parasitism, and projected final shell height based on data from the Choptank River (yellow, Kellogg and Paynter, unpublished data).

Predicted Reef Function:

Modeled oyster biomass on restored reefs generally increased through the year (Fig. 12), reflecting the modeled growth of individuals during the simulation (Figs. 10-11). Highest biomass was in Box 4, reflective of the high densities there (Table 4). Modeled mussel biomass was a function of oyster biomass, resulting in highest values in Boxes 1 and 4 (Fig. 12). Modeled tunicate biomass decreased with distance up the creek and followed the seasonal temperature cycle, reflecting the underlying formulation for this group. Modeled *Alitta* biomass followed a bimodal seasonal cycle reflective of the underlying formulation based on mussel biomass and temperature.

Simulated filtration rates for oysters, mussels, and tunicates all followed the seasonal temperature cycle, with values increasing through summer and peaking in early September (Fig. 13). Rates were generally greatest in the lower estuary and decreased towards the head (i.e., Box 5). As noted above, filtration was computed as a function of temperature, salinity, TSS, and DO; this was accomplished using dimensionless limitation functions expressing the fraction of maximum filtration realized as a function of each parameter (Ehrich and Harris 2015). Filtration was not predicted to be limited by TSS or DO during the entire year (limitation terms = 1),

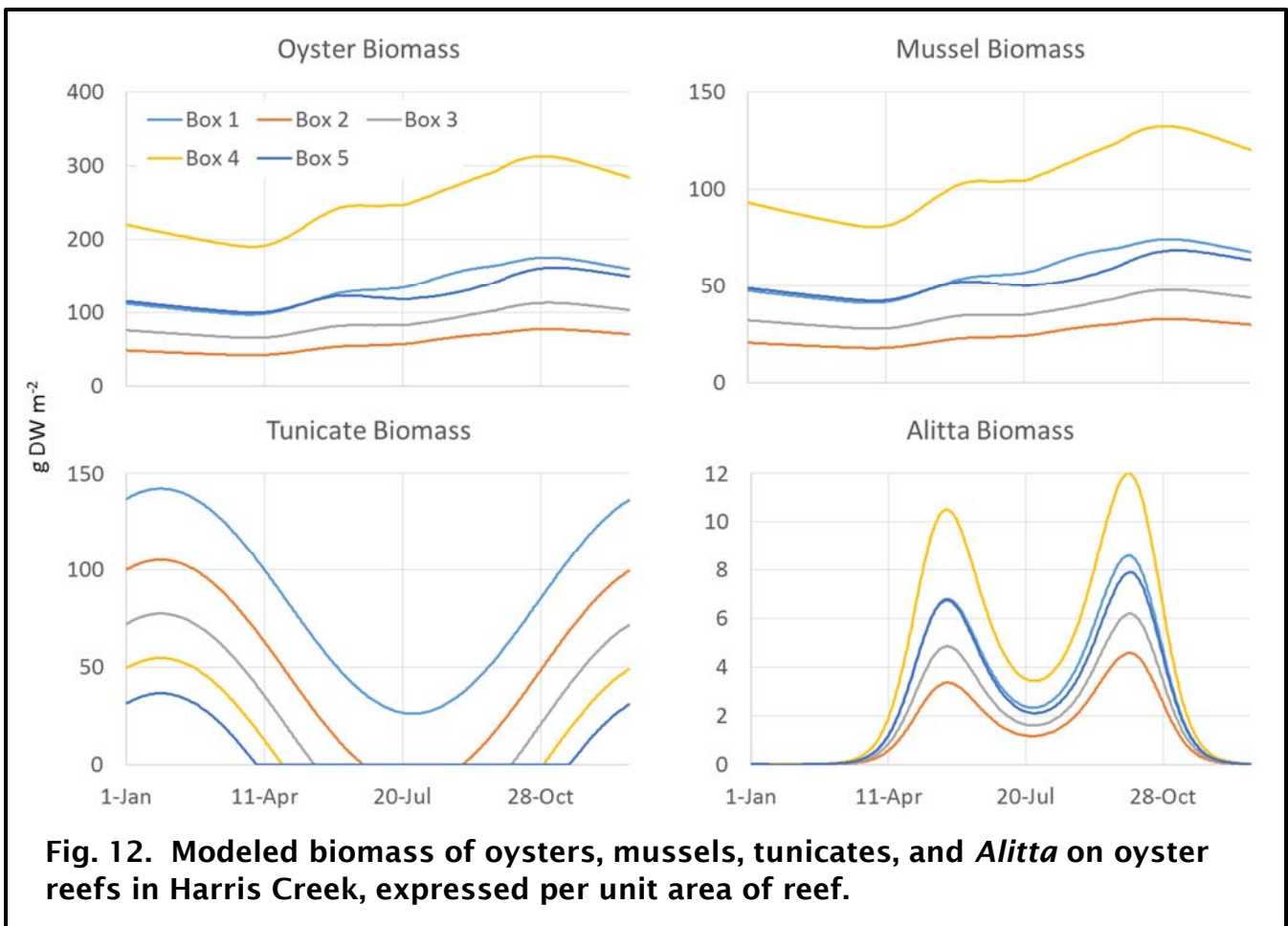


Fig. 12. Modeled biomass of oysters, mussels, tunicates, and *Alitta* on oyster reefs in Harris Creek, expressed per unit area of reef.

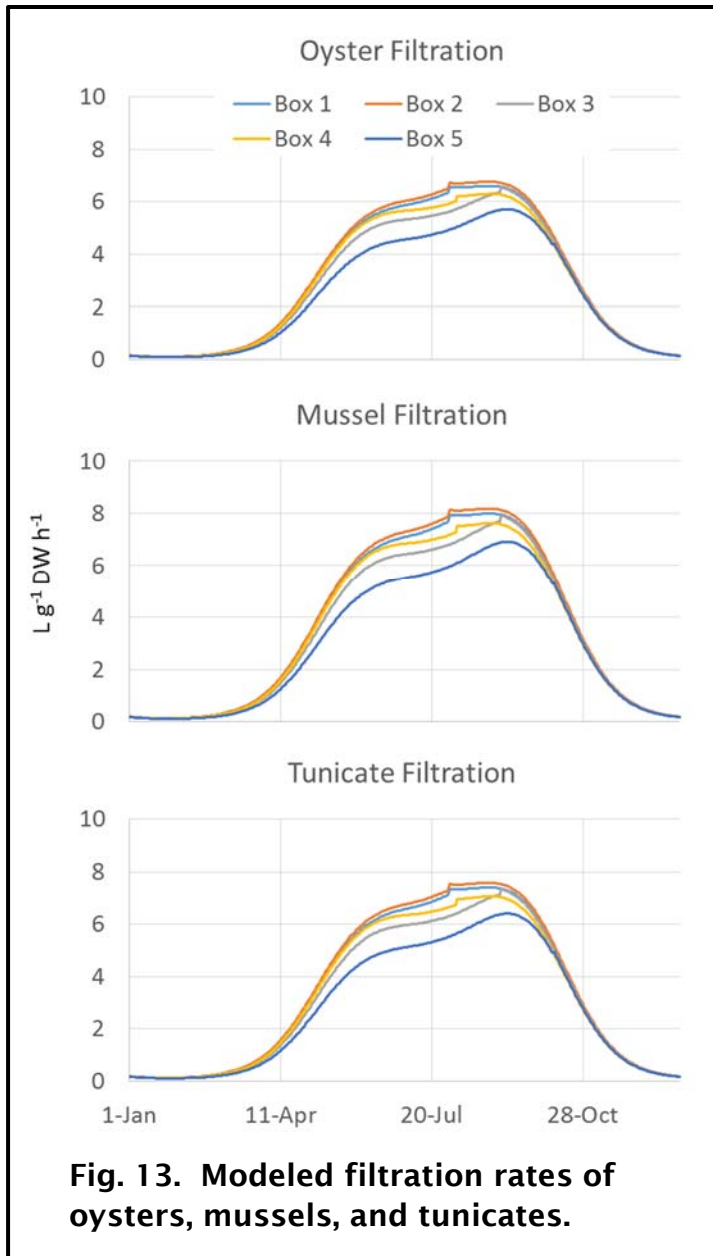
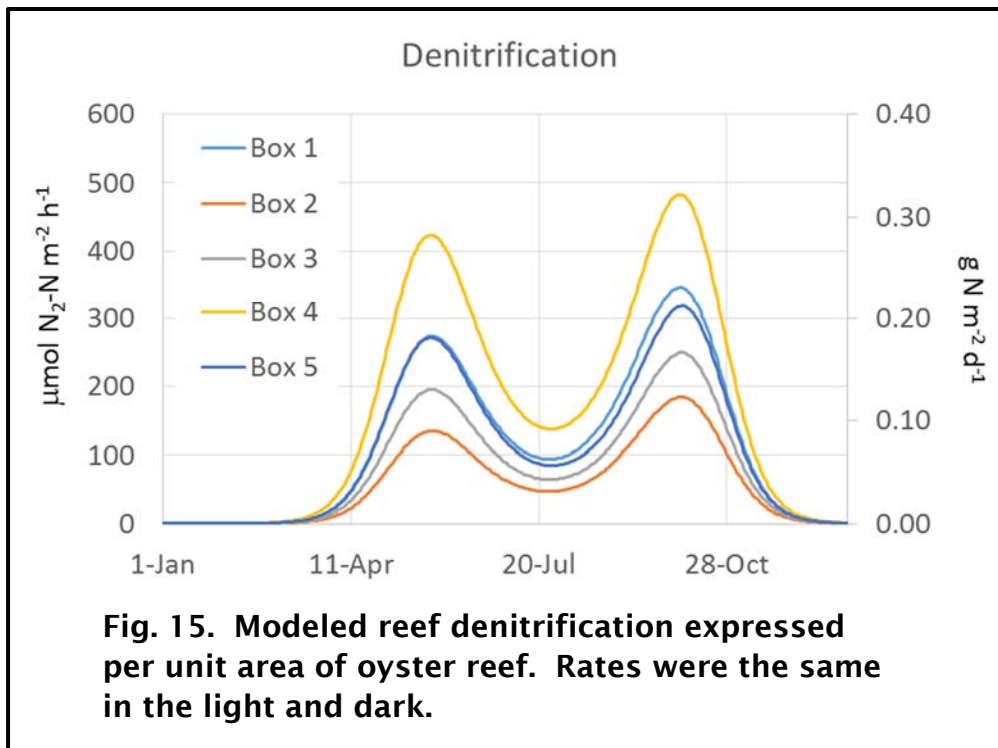
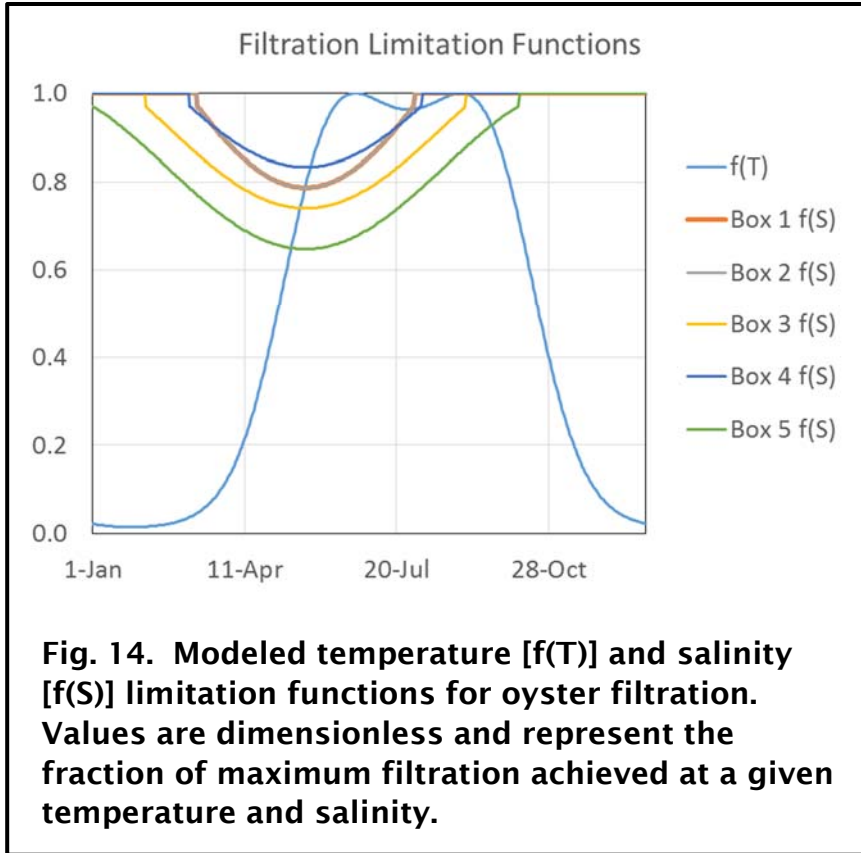
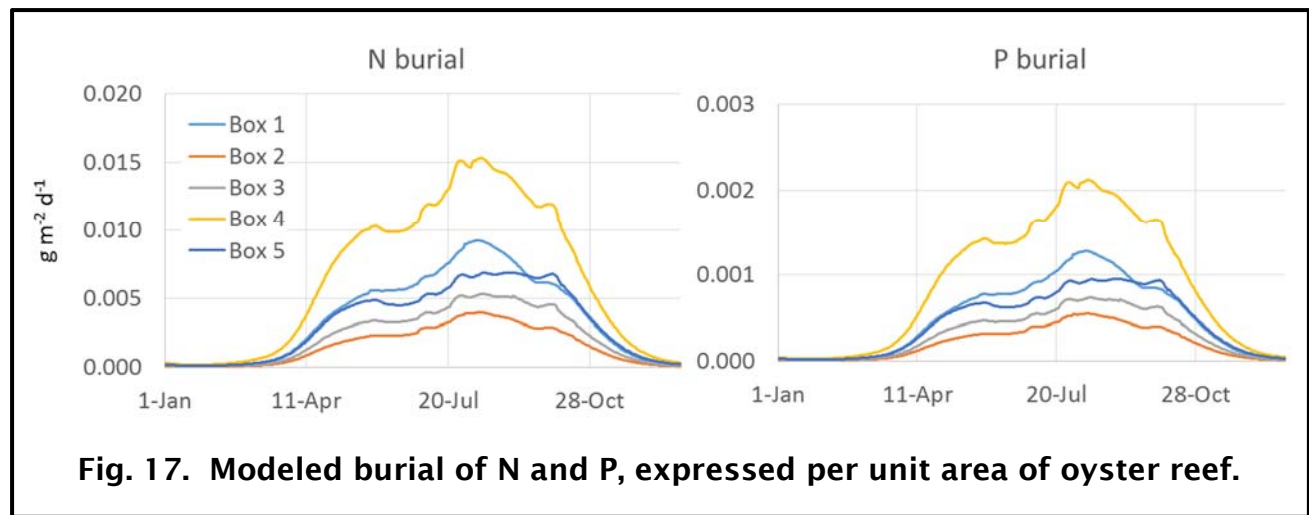
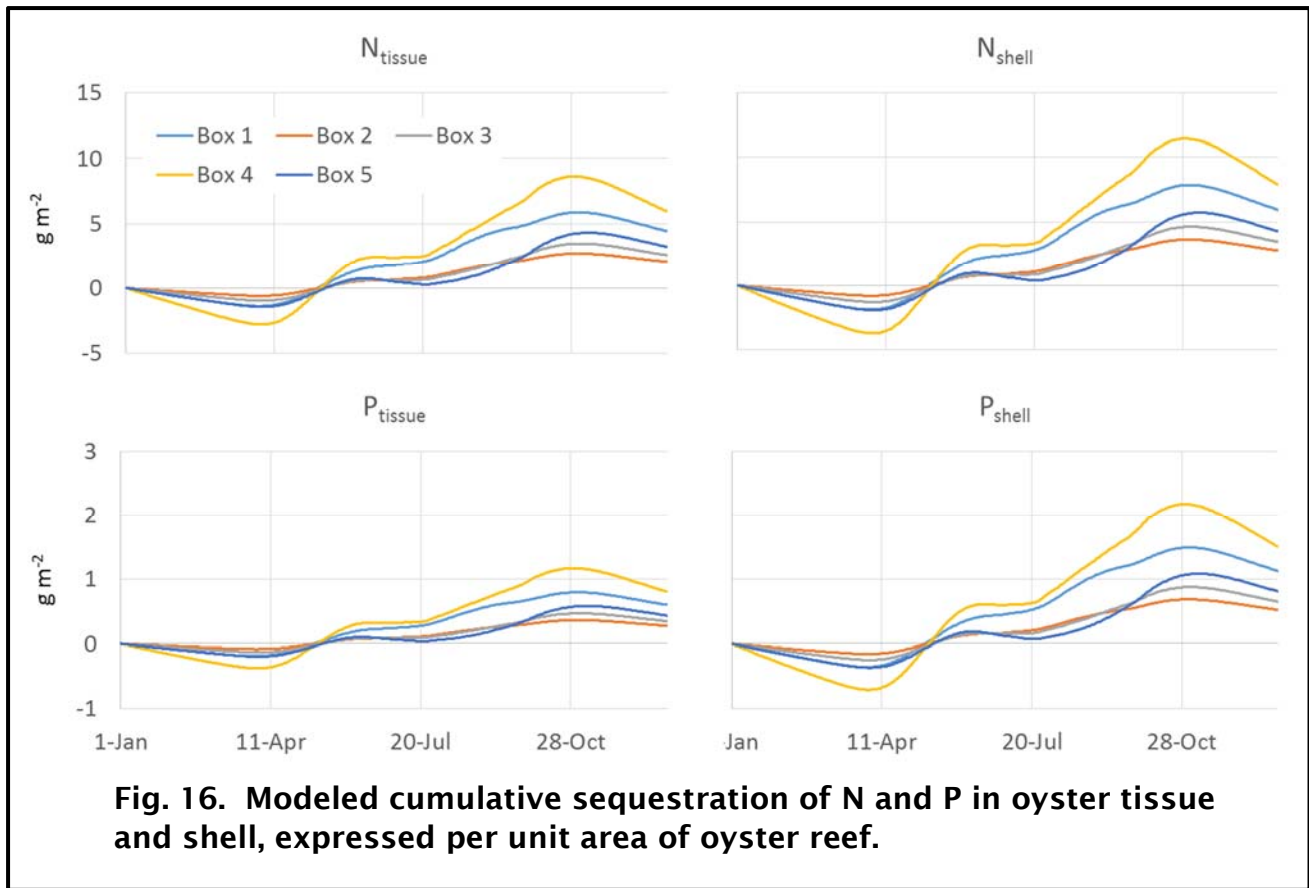


Fig. 13. Modeled filtration rates of oysters, mussels, and tunicates.

but temperature exerted a strong control throughout most of the year, with salinity becoming most limiting in late spring and summer, particularly in Box 5 (Fig. 14).

Modeled rates of reef denitrification were highest in Boxes 1, 4, and 5, where the highest biomass of *Alitta* was predicted, and followed the seasonal cycle of *Alitta* biomass (Fig. 15). Rates were in the range reported for a restored reef in the Choptank River (Kellogg et al. 2013), as well as the 2015 dataset collected in Harris Creek. Modeled sequestration of N in oyster tissue and shell (Fig. 16) was greatest in spring and fall during periods of accelerated oyster growth (see Figs. 10-11). These periods alternated with times of neutral or negative net sequestration. Sequestration in shell was higher than in tissue. Modeled sequestration of P in oyster tissue and shell was approximately an order of magnitude lower than that for N and showed the same seasonal pattern (Fig. 16). Modeled burial of N and P in sediments below oyster reefs followed a seasonal cycle with peak values during summer (Fig. 17).





To compute the impact of restored oyster reefs in Harris Creek on water quality, volume filtered, and removal of particulates and nutrients, the model was run using current reef area, oyster densities, and mean oyster sizes following the restoration (Table 4). The model was then re-run using values for the pre-restoration oyster population (Table 6) for comparison. Since the model function for tunicate biomass is not tied to oysters (see above), tunicates did not respond to the initial pre-restoration scenario. Since the current population of tunicates on the Harris Creek reefs has certainly been enhanced by the restoration, we re-ran the pre-restoration scenario without tunicates for a more realistic baseline. Results indicated that restored oyster reefs in Harris Creek have led to small decreases in chl-a and TSS concentrations (by 11.9 and 15.1%, respectively), and small increases in DO and Secchi depth (by 0.5 and 8.4%, respectively) at the system level (Table 11). However, absolute changes in these parameters were predicted to be very small despite the larger percent changes (Table 12).

Table 11. Mean annual percent change in water quality parameters in the post-restoration simulation relative to pre-restoration conditions. Positive values represent increases; negative values represent decreases. Values are given for each model box and for the system as a whole.

Parameter	Box 1	Box 2	Box 3	Box 4	Box 5	System
Chl-a	-8.8	-10.6	-12.4	-13.7	-13.9	-11.9
DO	0.2	0.4	0.6	0.6	0.7	0.5
TSS	-9.6	-13.1	-16.1	-18.0	-18.4	-15.1
Secchi	4.6	7.3	8.3	9.7	12.3	8.4

Table 12. Mean annual absolute change in water quality parameters in the post-restoration simulation relative to pre-restoration conditions. Positive values represent increases; negative values represent decreases. Values are given for each model box and for the system as a whole.

Parameter	Box 1	Box 2	Box 3	Box 4	Box 5	System
Chl-a, $\mu\text{g l}^{-1}$	-0.9	-1.4	-1.6	-1.6	-2.7	-1.6
DO, mg l^{-1}	0.02	0.04	0.05	0.05	0.07	0.04
TSS, mg l^{-1}	-1.0	-1.6	-1.9	-2.0	-3.5	-2.0
Secchi, m	0.04	0.06	0.06	0.08	0.07	0.06

Values in all remaining analyses reflect removals by the restored reefs only; i.e., the small effects of the pre-restoration oyster population have been removed. Oysters were predicted to filter the greatest amount of water annually, followed by mussels and then tunicates (Table 13). As noted previously, our estimates for tunicate filtration capacity likely underestimate actual capacity because the tunicate filtration scales with oyster filtration but tunicates can actively filter at temperatures below those at which oysters cease filtration. Total volume filtered varied over the annual cycle with highest rates in summer (Fig. 18). While the percent of creek volume filtered by restored reefs reached over 16% d⁻¹ at peak rates, over the full annual cycle daily filtration was about half that, with an average of 7.3% d⁻¹ (Table 14). We note that these filtration rates have been corrected as described above using the ‘p-value’ to constrain filtration to produce reasonable growth, so rates are lower than those computed using filtration rate equations directly from the literature.

Oysters similarly removed the greatest amount of chl-a annually, followed by mussels and tunicates (Table 15). Reefs were estimated to remove an average of 6.7% of the creekwide standing stock of chl-a each day, with rates varying widely over the annual cycle (Table 16, Fig. 19). Results were similar for removal of TSS by restored reefs, with respect to total annual removals (Table 17) and daily removal of the creekwide standing stock (Table 18, Fig. 20).

Denitrification was the dominant mechanism by which restored reefs were predicted to remove nitrogen from the system, followed by sequestration in shells, sequestration in tissues, and burial (Table 19). Removals were greatest in Box 1 and decreased with distance up-creek (Fig. 21). Sequestration in shells was the dominant mechanism by which reefs removed phosphorus, followed by sequestration in tissues and burial (Table 21). As for nitrogen, removals were greatest in Box 1 and decreased up-creek (Fig. 22).

Annual removals of N, P, TSS, and organic carbon (OC) by oyster reefs were compared to simulated inputs from various sources, including the watershed, atmosphere (N only), exchange across the mouth with the Choptank River, and internal phytoplankton net primary production (NPP, OC only) (Table 21). Reefs appear able to remove far in excess of current loading rates to Harris Creek from the watershed and atmospheric deposition. However, this is due to the small, groundwater-driven nature of the watershed and small surface area of the estuary. Most material loading to the creek comes via exchange with the Choptank River, and reefs are able to remove a much smaller fraction of these inputs. That said, removal of ~22% of TSS coming from the Choptank and nearly one quarter of phytoplankton production within the creek is substantial. Overall restored reefs are able to remove less than 10% of the inputs of N, P, and OC, but 22% of TSS.

Table 13. Modeled annual filtration by restored oyster reefs in each box and for the entire system, expressed x 10⁶ m³ y⁻¹.

	Box 1	Box 2	Box 3	Box 4	Box 5	System
Oysters	335	64	71	57	7	535
Mussels	172	33	36	29	4	274
Tunicates	136	20	5	0	0	161
Total	643	117	112	87	11	969

Table 14. Modeled daily filtration expressed as a percent of volume in each box and for the entire system (i.e., % d⁻¹). Summary statistics were computed from daily values over the one-year simulation.

	Oysters	Mussels	Tunicates	Total
Average	4.0	2.1	1.2	7.3
Median	3.3	1.7	1.2	6.8
Minimum	0.1	0.1	0.2	0.3
Maximum	9.6	4.9	2.5	16.5

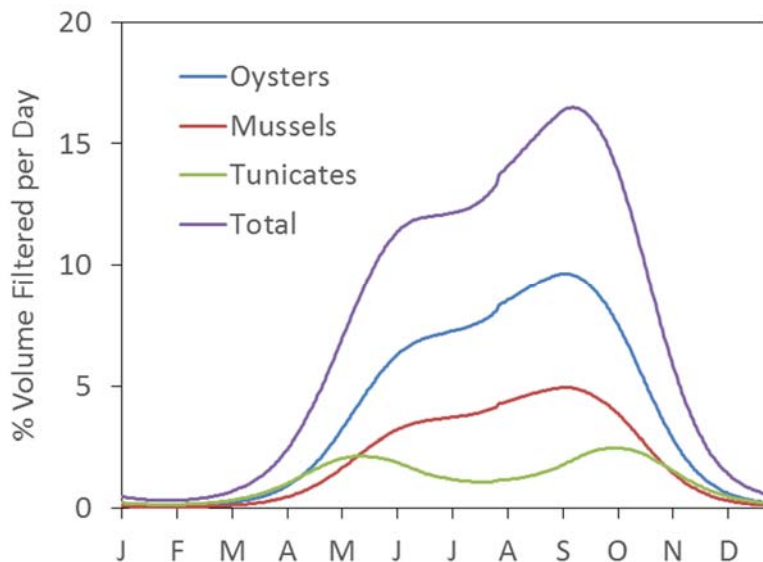


Fig. 18. Modeled daily filtration by restored reefs expressed as a percent of Harris Creek volume.

Table 15. Modeled annual removal of chlorophyll-a in each box and for the entire system, expressed x 10⁶ g y⁻¹.

	Box 1	Box 2	Box 3	Box 4	Box 5	System
Oysters	2.9	0.7	0.7	0.5	0.1	4.9
Mussels	1.5	0.3	0.4	0.3	0.1	2.5
Tunicates	1.3	0.2	0.1	0.0	0.0	1.6
Total	5.7	1.2	1.1	0.8	0.2	9.0

Table 16. Modeled daily removal of chl-a expressed as a percent of total mass in the system (i.e., % d⁻¹). Summary statistics were computed from daily values over the one-year simulation.

	Oysters	Mussels	Tunicates	Total
Average	3.7	1.9	1.1	6.7
Median	3.0	1.5	1.1	6.3
Minimum	0.1	0.1	0.1	0.3
Maximum	8.7	4.5	2.2	14.7

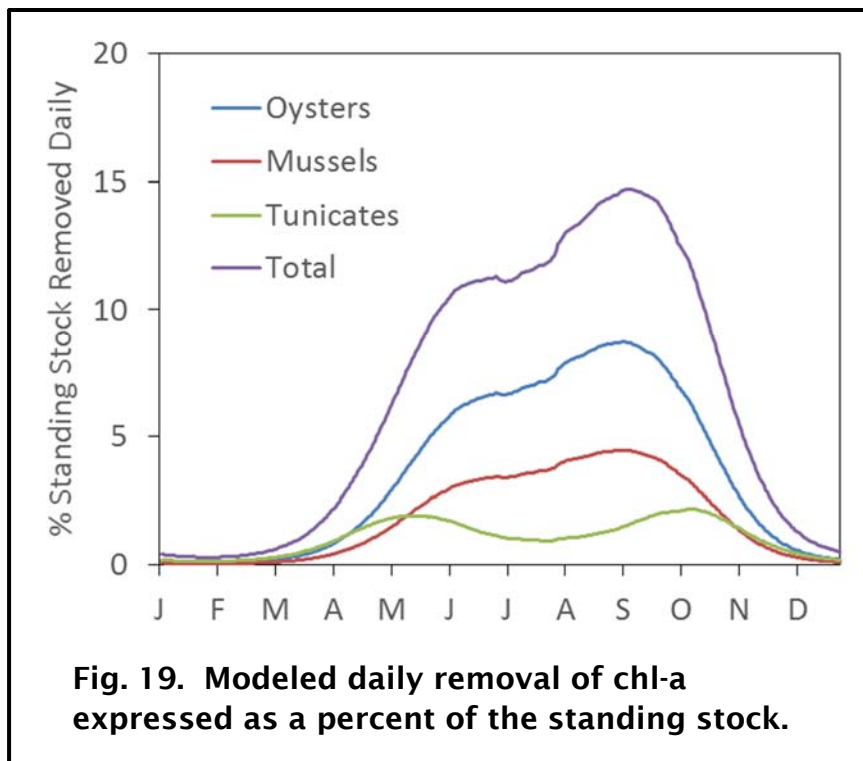


Table 17. Modeled annual removal of TSS in each box and for the entire system, expressed x 10⁶ g y⁻¹.

	Box 1	Box 2	Box 3	Box 4	Box 5	System
Oysters	2,843	600	618	438	97	4,596
Mussels	1,456	307	317	224	50	2,354
Tunicates	1,194	202	53	5	1	1,455
Total	5,493	1,109	988	667	148	8,406

Table 18. Modeled daily removal of TSS expressed as a percent of total mass in the system (i.e., % d⁻¹). Summary statistics were computed from daily values over the one-year simulation.

	Oysters	Mussels	Tunicates	Total
Average	3.8	1.9	1.1	6.8
Median	3.1	1.6	1.1	6.4
Minimum	0.1	0.1	0.1	0.3
Maximum	9.1	4.7	2.3	15.6

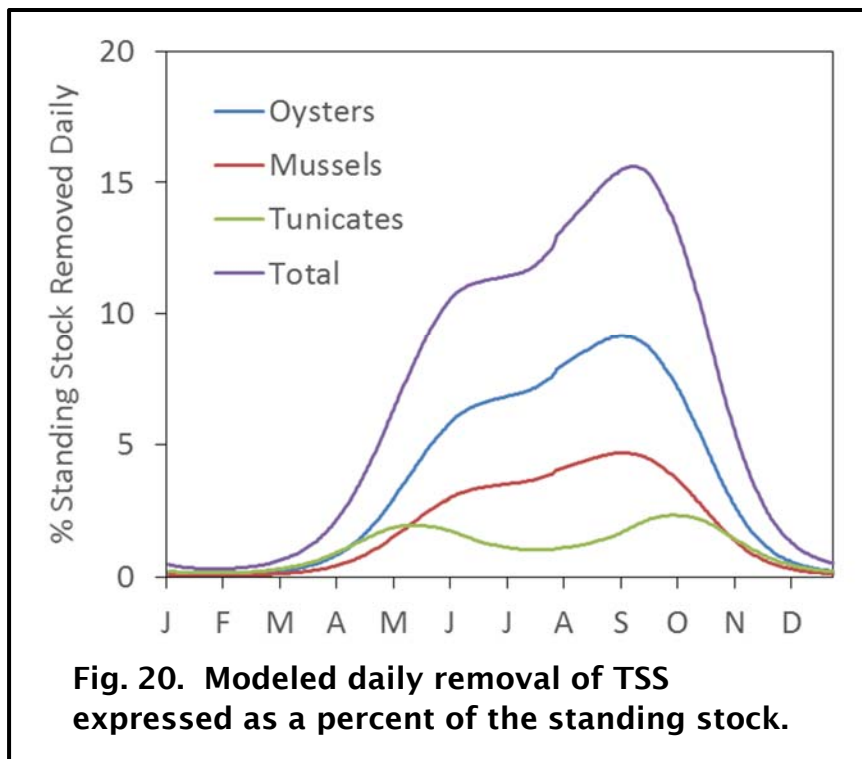


Table 19. Modeled annual removal of N in each box and for the entire system, expressed $\times 10^6 \text{ g y}^{-1}$.

	Box 1	Box 2	Box 3	Box 4	Box 5	System
Denitrification	18.9	5.1	5.2	2.6	0.7	32.5
Tissue	2.8	0.7	0.6	0.3	0.1	4.5
Shell	3.8	0.9	0.8	0.4	0.1	6.0
Burial	0.9	0.2	0.2	0.2	0.0	1.5
Total	26.4	6.9	6.9	3.4	1.0	44.5

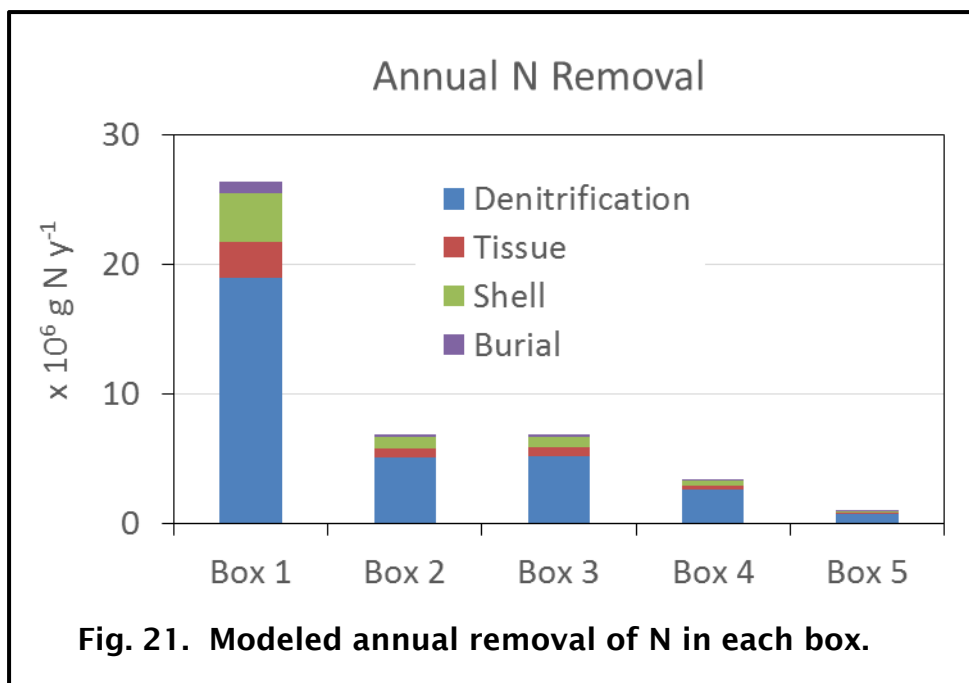


Table 20. Modeled annual removal of P in each box and for the entire system, expressed $\times 10^6 \text{ g y}^{-1}$.

	Box 1	Box 2	Box 3	Box 4	Box 5	System
Tissue	0.38	0.09	0.08	0.04	0.01	0.61
Shell	0.72	0.18	0.16	0.07	0.02	1.14
Burial	0.12	0.03	0.03	0.02	0.00	0.21
Total	1.23	0.30	0.27	0.13	0.04	1.96

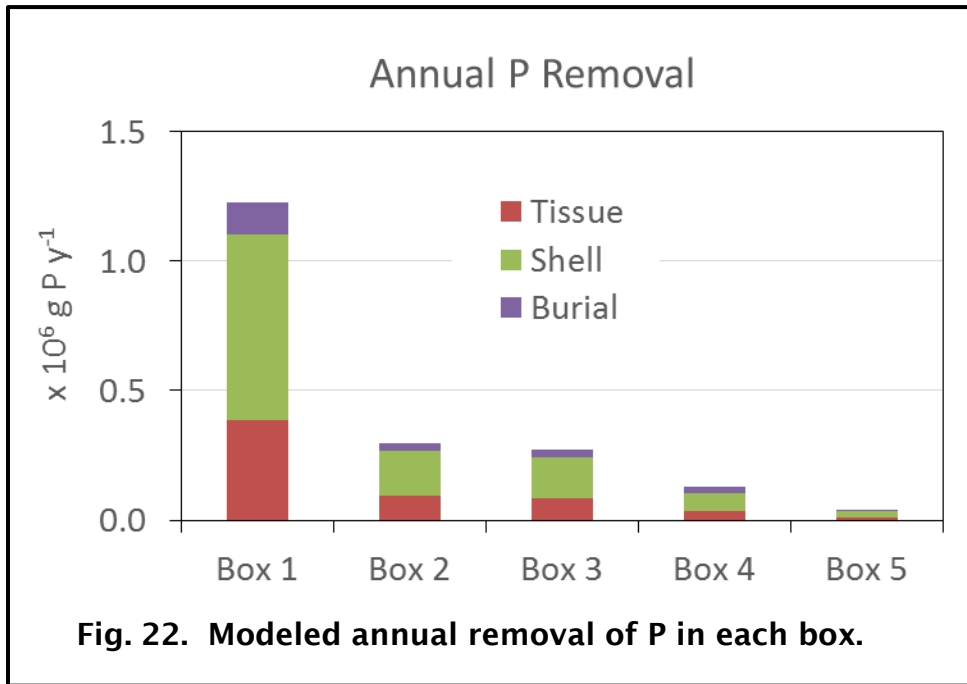


Table 21. Modeled percent of annual inputs of N, P, TSS, and organic carbon from various sources removed by restored oyster reefs in Harris Creek. ‘Choptank River’ refers to the input of materials across the mouth of Harris Creek due to tidal exchange.

	N	P	TSS	OC
Watershed	208	138	1230	322
Atmosphere	474			
Choptank River	4.7	8.2	22.4	12.9
Phytoplankton NPP				24.5
Total	4.6	7.8	22.0	8.3

Online Interface

The original online interface has been enhanced and the revised model is served online through the VIMS Coastal Systems Ecology and Modeling Program (CSEMP) website. The direct link to the model is:

exchange.iseesystems.com/public/markbrush/harris-creek-model-v2

or it can be accessed through the CSEMP online modeling site:

www.vims.edu/research/departments/bio/programs/sem/models/index.php

The online model completes an annual simulation in a matter of seconds. As in the first version of the model, the first several pages of the interface describe the model and input data, and are followed by the Scenario Analysis Page in which the user can run the model or alter user-defined values for reef acres, oyster density, and oyster weight (Fig. 23). The user can also enter nutrient trading credits (\$ pound⁻¹) to compute the economic value of the simulated nutrient removals.

As noted above, current default values were derived from the 2017 Harris Creek Oyster Restoration Blueprint Geodatabase, and represent our best estimates of values through 2016. Areas, densities, and weights can be entered for any point in time for which the user has data; care needs to be taken when entering densities as the model does not assume mortality over time. Accuracy of the estimated TMDL-related benefits of oyster reef restoration in Harris Creek will depend heavily upon the accuracy of the values entered by the user.

1. Specify the acres of restored oyster reefs in each spatial element.

Acres of Restored Reefs	
	Value
Oyster acres[1]	168.6
Oyster acres[2]	88.5
Oyster acres[3]	65.6
Oyster acres[4]	17.9
Oyster acres[5]	6.9

2. Specify the density of restored oysters (#/acre) in each spatial element.

Restored Oyster Density	
	Value
Oyster density[1]	477529
Oyster density[2]	224601
Oyster density[3]	284090
Oyster density[4]	696060
Oyster density[5]	370288

3. Specify the average tissue weight (g dry) of restored oysters in each spatial element.

Mean Oyster Weight	
	Value
Oyster DWio[1]	0.95
Oyster DWio[2]	0.87
Oyster DWio[3]	1.08
Oyster DWio[4]	1.28
Oyster DWio[5]	1.26

4. Optional: Specify the value of nutrient removal (\$/pound):

Nutrient Credits	
	Value
N price	0
P price	0

Fig. 23. Screen shots of the simple, user-friendly interface for altering model parameters.

Once the model is run, the user can navigate to the Model Output Dashboard to select the parameter(s) they wish to view output for, or to export model output as .csv files for importing into a spreadsheet program. Appendix B provides screen shots and descriptions of each page in the online model; some of the screenshots contain output from a sample model run.

Summary

The revised Harris Creek Model includes a number of enhancements relative to the original version. This includes incorporation of forcing and calibration data through 2016, addition of a new dataset for use in calibration (MDDNR calibration cruise data), expansion of the number of water quality parameters used in calibration, and collection of BMA chl-a data to calibrate that portion of the model. The lack of TSS and BMA chl-a data were highlighted in our previous report as significant sources of uncertainty in model calibration (Kellogg et al. 2014). Hypsography was also updated with a much more finely resolved bathymetric dataset from the USGS (2016).

The model now includes all restored reefs through 2016, and current (2016-17) estimates of reef area, oyster density, and mean oyster weight. We have estimated the pre-restoration oyster population within the creek to generate a baseline simulation. The model now makes use of two independent methods to estimate annual oyster growth of both tissue and shell for use in calibration. Perhaps most significantly, we were able to use a new dataset of macrofaunal biomass and biogeochemical fluxes collected within Harris Creek to revise our formulation for denitrification and to add filtration impacts from two dominant reef-associated organisms, the hooked mussel *Ischadium recurvum* and the sea squirt *Molgula manhattensis*.

The completed model was calibrated to reproduce observed oyster growth, and successfully reproduced the available water quality monitoring data. The completed model was used to provide current estimates of volume filtration and removal of particulates and nutrients by restored reefs. Reefs were predicted to have had small, positive impacts on water quality within the creek. Water filtration and removal of chl-a and TSS were strongly seasonal, and on average the reefs are able to filter and remove modest amounts (< 10%) of total creek volume and particulate stocks, respectively. Reef-associated macrofauna such as mussels and tunicates substantially increase overall reef filtration and particulate removal capacity. Denitrification was predicted to be the dominant reef-associated N removal process, followed by sequestration in shells, sequestration in tissues, and burial; results followed the same sequence for P (excluding denitrification). Restored reefs were predicted to remove far greater than 100% of watershed and

atmospheric loads to the creek, but generally <10% of total inputs (22% for TSS) since loads to Harris Creek are dominated by exchanges with the Choptank River.

Despite the improvements in the revised model related to incorporation of new data, the model would still benefit from continued addition of new water quality data, particularly for TSS and nutrients, and for any parameter in boxes where data currently do not exist. Additional macrofaunal and denitrification data could enable us to relate both tunicate biomass and denitrification back to oyster biomass (rather than *Alitta* biomass for the latter), as they are currently uncoupled which limits the ability of the model to predict changes in these components as a function of oyster restoration. Additional data would also help constrain the relationships developed for computing macrofaunal biomass and denitrification, which are currently characterized by high uncertainty. As noted in our previous report, there are no direct estimates of N and P deposition associated with restored reefs in the Chesapeake, or of the rate of burial. Data on these processes would be very helpful in improving and constraining model predictions.

The successful model revision indicates that the model is a valid tool for estimating the TMDL-related benefits of oyster restoration in Harris Creek and for comparing various restoration scenarios. The reduced complexity nature of the Harris Creek Model makes this tool amenable to updating as additional data become available. The model will continue to be maintained online through the VIMS Coastal Systems Ecology and Modeling Program and we envision uploading future versions of the model as it is improved through inclusion of new research and monitoring data. The reduced complexity approach also makes the model readily applicable to other systems in the Chesapeake Bay and on the Eastern Shore.

Outreach Activities

Kellogg and Brush participated in the Harris Creek Water Column Habitat Pilot Project Advisory Group, 2016-18, coordinated by the Mid Atlantic Regional Association Coastal Ocean Observing System (MARACOOS) and NOAA Chesapeake Bay Office (NCBO), informing participants about the model and generating output for discussion. Data from or information about this project have also been presented at meetings attended by resource managers, restoration practitioners and researchers. Presentations to date include:

Kellogg, M.L., J.C. Cornwell, P.G. Ross, K.T. Paynter, M.W. Luckenbach, M.S. Owens, J.C. Dreyer, M. Pant, C. Turner, A. Birch, E. Smith, S. Fate. 2018, Quantifying the benefits of tributary-scale oyster reef restoration. 2018 Chesapeake Community Research & Modeling Symposium, Annapolis, MD.

- Brush, M.J. 2017. Quantifying the ecosystem-level benefits and trade-offs associated with Eastern oyster restoration in contrasting sub-estuaries. Coastal and Estuarine Research Federation biennial conference, Providence, RI.
- Brush, M.J. 2016. Modeling through the macroscope: reduced complexity models for coastal ecosystem science and management. Invited keynote research seminar as part of the workshop, Modelling Estuarine Ecosystems. Atlantic Canada Coastal and Estuarine Science Society annual meeting, Charlottetown, PEI.
- Brush, M.J. and M.L. Kellogg. 2016. Uncertainty in modeled estimates of nutrient removal from oyster restoration. Chesapeake Modeling Symposium 2016, Chesapeake Community Modeling Program, Williamsburg, VA.
- Brush, M.J. and M.L. Kellogg. 2014. A user-friendly, online model for estimating the TMDL-related benefits of oyster reef restoration in Harris Creek, MD. Chesapeake Modeling Symposium 2014, Chesapeake Community Modeling Program, Annapolis, MD.
- Brush, M.J., M.L. Kellogg, M.A. Kuschner, and E.E. Skeehan. 2016. Linking bivalve and seagrass models with reduced complexity watershed and estuarine models to support nutrient management, aquaculture production, and climate mitigation. Chesapeake Modeling Symposium 2016, Chesapeake Community Modeling Program, Williamsburg, VA.
- Brush, M.J., M.L. Kellogg, and E.E. Skeehan. 2015. A user-friendly, online model for estimating the ecosystem impact of oyster restoration. National Shellfisheries Association annual meeting, Monterey, CA.
- Kellogg M.L. 2013. Oysters, reef restoration and water quality: A Chesapeake Bay perspective. 12th Annual Ronald C. Baird Sea Grant Science Symposium, Warwick, RI.
- Kellogg, M.L., M.J. Brush, and Y. Lee. 2014. Challenges in modeling the water quality benefits of oyster reef restoration: Harris Creek, MD. National Shellfisheries Association 106th annual meeting, Jacksonville, FL.

Literature Cited

- Boynton, W.R., J.H. Garber, R. Summers, and W.M. Kemp. 1995. Inputs, transformations, and transport of nitrogen and phosphorus in Chesapeake Bay and selected tributaries. *Estuaries* 18(1B):285-314.
- Brush, M.J. and S.W. Nixon. 2017. A reduced complexity, hybrid empirical-mechanistic eutrophication and hypoxia model for shallow marine ecosystems. Chapter 4 in: Justic, D., K.A. Rose, R.D. Hetland, and K. Fennel (eds.), *Modeling coastal*

hypoxia: numerical simulations of patterns, controls and effects of dissolved oxygen dynamics. Springer.

- Brush, M.J., J.W. Brawley, S.W. Nixon, and J.N. Kremer. 2002. Modeling phytoplankton production: problems with the Eppley curve and an empirical alternative. *Marine Ecology Progress Series* 238:31-45.
- Cerco, C.F. and M.R. Noel. 2005. Evaluating ecosystem effects of oyster restoration in Chesapeake Bay. Report to the Maryland Department of Natural Resources, Annapolis, MD.
- Cerco, C.F. and M.R. Noel. 2007. Can oyster restoration reverse cultural eutrophication in Chesapeake Bay? *Estuaries and Coasts* 30(2):331–343.
- Coen, L., R. Brumbaugh, D. Bushek, R. Grizzle, M. Luckenbach, M. Posey, S. Powers, and S. Tolley. 2007. Ecosystem services related to oyster restoration. *Marine Ecology Progress Series* 341:303–307.
- Cornwell, J.C., Kellogg M.L., Owens M.S., Luckenbach M.W., J.C. Dreyer, C. Turner, M. Pant. 2016. Integrated assessment of oyster reef ecosystem services: Quantifying denitrification rates and nutrient fluxes. Final report to: National Oceanic and Atmospheric Administration’s Chesapeake Bay Office, 19 pp.
- Duarte, C.M., J.S. Amthor, D.L. DeAngelis, L.A. Joyce, R.J. Maranger, M.L. Pace, J. Pastor, and S.W. Running. 2003. The limits to models in ecology. Pp. 437-451 in: Canham, C.D., J.J. Cole, and W.K. Lauenroth (eds.), *Models in Ecosystem Science*. Princeton University Press, Princeton, NJ.
- Ehrich, M.K. and L.A. Harris. 2015. A review of existing eastern oyster filtration rate models. *Ecological Modelling* 297:201–212.
- Fulford, R.S., D.L. Breitburg, R.I.E. Newell, W.M. Kemp, and M. Luckenbach. 2007. Effects of oyster population restoration strategies on phytoplankton biomass in Chesapeake Bay: a flexible modeling approach. *Marine Ecology Progress Series* 336: 43–61.
- Ganju, N.K., M.J. Brush, B. Rashleigh, A.L. Aretxabaleta, P. del Barrio, J.S. Grear, L.A. Harris, S.J. Lake, G. McCardell, J. O’Donnell, D.K. Ralston, R.P. Signell, J.M. Testa, and J.M.P. Vaudrey. 2016. Progress and challenges in coupled hydrodynamic-ecological estuarine modeling. *Estuaries and Coasts* 39:311–332.
- Kellogg, M.L., K.T. Paynter, P.G. Ross, J.C. Dreyer, C. Turner, M. Pant, A. Birch, E. Smith. 2016. Integrated assessment of oyster reef ecosystem services: Macrofauna utilization of restored oyster reefs. Final report to: National Oceanic and

Atmospheric Administration's Chesapeake Bay Office, 27 pp.

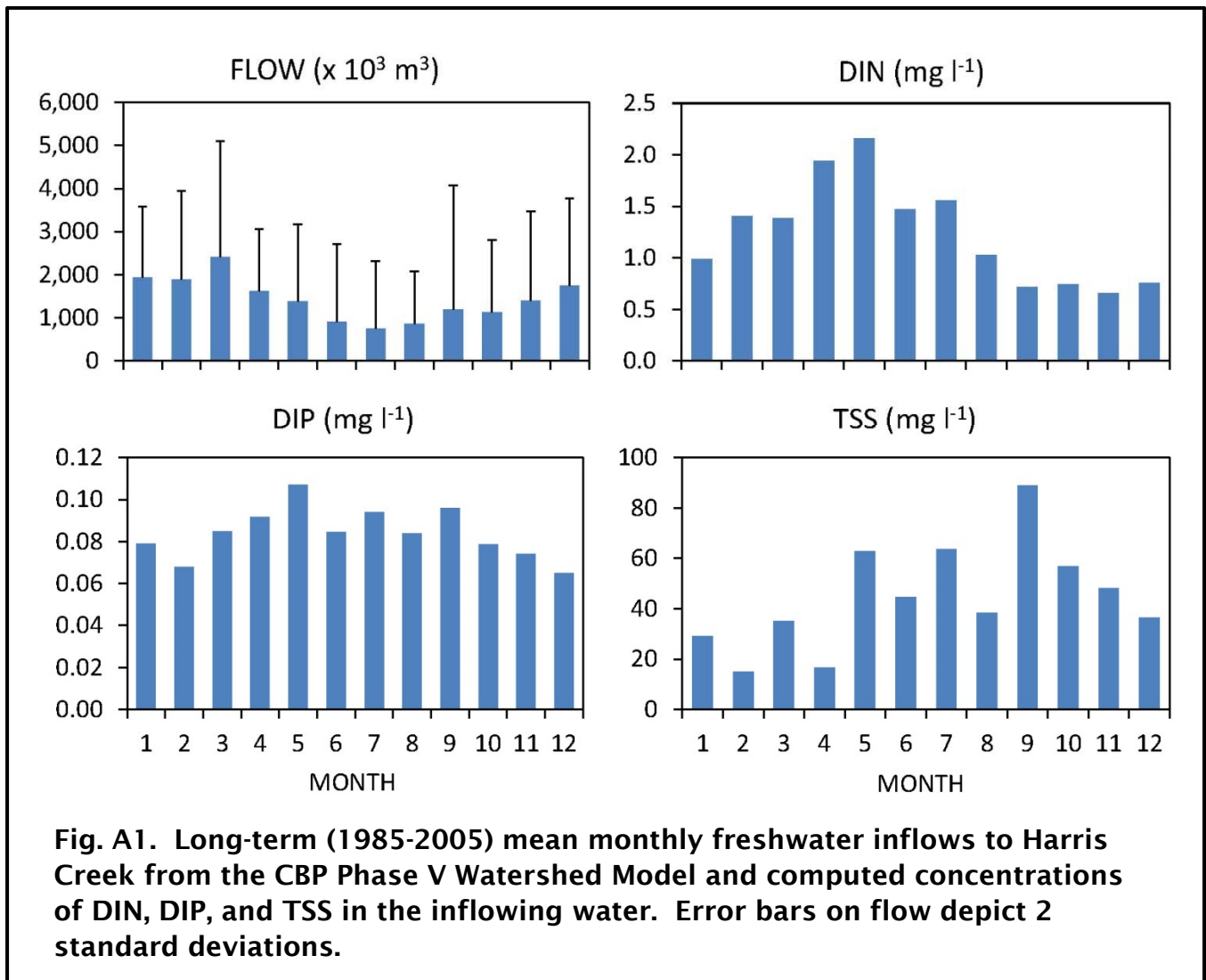
- Kellogg, M.L., M.J. Brush, E.W. North, and Y. Lee. 2014a. A model for estimating the TMDL-related benefits of oyster reef restoration in Harris Creek, MD. Final report, National Fish and Wildlife Foundation and Oyster Recovery Partnership, Inc.
- Kellogg, M.L., A.R. Smyth, M.W. Luckenbach, R.H. Carmichael, B.L. Brown, J.C. Cornwell, M.F. Piehler, M.S. Owens, D.J. Dalrymple, C.B. Higgins. 2014b. Use of oysters to mitigate eutrophication in coastal waters. *Estuarine, Coastal and Shelf Science* 151: 156-158.
- Kellogg, M. L., J. C. Cornwell, M. S. Owens, and K. T. Paynter. 2013. Denitrification and nutrient assimilation on a restored oyster reef. *Marine Ecology Progress Series* 480: 1-19.
- Liddel, M.K. 2008. A von Bertalanffy model for the estimation of oyster (*Crassostrea virginica*) growth on restored oyster reefs in the Chesapeake Bay. Ph.D. dissertation, University of Maryland, College Park.
- Lorenzen, C. 1967. Determination of chlorophyll and phaeopigments: spectrophotometric equations. *Limnology and Oceanography* 12: 343-346.
- Newell, R.I.E. 1988. Ecological changes in Chesapeake Bay: Are they the result of overharvesting the American oyster, *Crassostrea virginica*? Understanding the Estuary: Advances in Chesapeake Bay Research. *Proceedings of a Conference* 29:1-11.
- Newell, R. I. E. 2004. Ecosystem influences of natural and cultivated populations of suspension-feeding bivalve molluscs: A review. *Journal of Shellfish Research* 23:51-61.
- Newell R., T. R. Fisher, R. Holyoke, J. Cornwell. 2005. Influence of eastern oysters on nitrogen and phosphorus regeneration in Chesapeake Bay, USA. In: R Dame, S Olenin (eds) *The Comparative Roles of Suspension-Feeders in Ecosystems*. Kluwer, Netherlands
- NOAA. 2016. Analysis of monitoring data from Harris Creek Sanctuary oyster reefs: Data on the first 102 acres/12 reefs restored. 70pp.
- NOAA. 2017. 2016 Oyster reef monitoring report: Analysis of data from large-scale sanctuary oyster restoration projects in Maryland. 142 pp.

- North, E.W., W. Long, Z. Schlag, and S. Suttles. 2012. Native Oyster Recovery: Hydrodynamic and Larval Transport Modeling in Harris Creek. Final report to Army Corps of Engineers, March 2, 2012. 37 pp.
- NRC (National Research Council). 2000. Clean coastal waters: understanding and reducing the effects of nutrient pollution. National Academy Press, Washington, DC.
- Paynter, K., H. Lane and A. Michaelis. 2013. Paynter Lab Annual Monitoring and Research Summary 2012. Submitted to the Oyster Recovery Partnership. 100 pp.
- Rose, J.M., S.B. Bricker, M.A. Tedesco, and G.H. Wikfors. 2014. A role for shellfish aquaculture in coastal nitrogen management. *Environmental Science & Technology* 48:2519–2525.
- Shchepetkin, A.F., and J.C. McWilliams. 1980. The Regional Ocean Modeling System: A split-explicit, free-surface, topography following coordinates ocean model. *Ocean Modelling*. 9:347-404.
- US Army Corps of Engineers – Baltimore and Norfolk Districts. 2012. Chesapeake Bay Oyster Recovery: Native Oyster Restoration Master Plan, Maryland and Virginia.
http://www.nab.usace.army.mil/Portals/63/docs/Environmental/Oysters/CB_OysterMasterPlan_Oct2012_FINAL.pdf. Accessed 28 Jun 2014.
- US Environmental Protection Agency. 2010. Chesapeake Bay Total Maximum Daily Load for Nitrogen, Phosphorus and Sediment.
<http://www.epa.gov/reg3wapd/tmdl/ChesapeakeBay/tmdlexec.html>. Accessed 28 Jun 2014.
- US Environmental Protection Agency. 2018. Appendix A: Recognizing pollutant reductions via in-situ oyster filtration under the Clean Water Act.
https://oysterrecovery.org/wp-content/uploads/2015/10/Update-on-Oyster-BMP-Expert-Panel-2nd-Report_2-1-18_Final.pdf. Accessed 10 Jun 2018.
- USGS. 2016. Topobathymetric model for Chesapeake Bay region – District of Columbia, States of Delaware, Maryland, Pennsylvania, and Virginia, 1859 to 2015. Danielson, J. and D. Tyler, USGS Earth Resources Observation & Science Center, Science and Applications Branch, Sioux Falls, SD.

Versar, Inc. 2012. An assessment of oyster resources in Harris Creek and Little Choptank River, Chesapeake Bay. Draft final report to the NOAA Chesapeake Bay Office, Annapolis, MD. Versar, Inc., Columbia, MD.

Wetzel, R.L. and H.A. Neckles. 1986. A model of *Zostera marina* L. photosynthesis and growth: simulated effects of selected physical-chemical variables and biological interactions. *Aquatic Botany* 26:307–323.

Appendix A: Model Inputs and Calibration



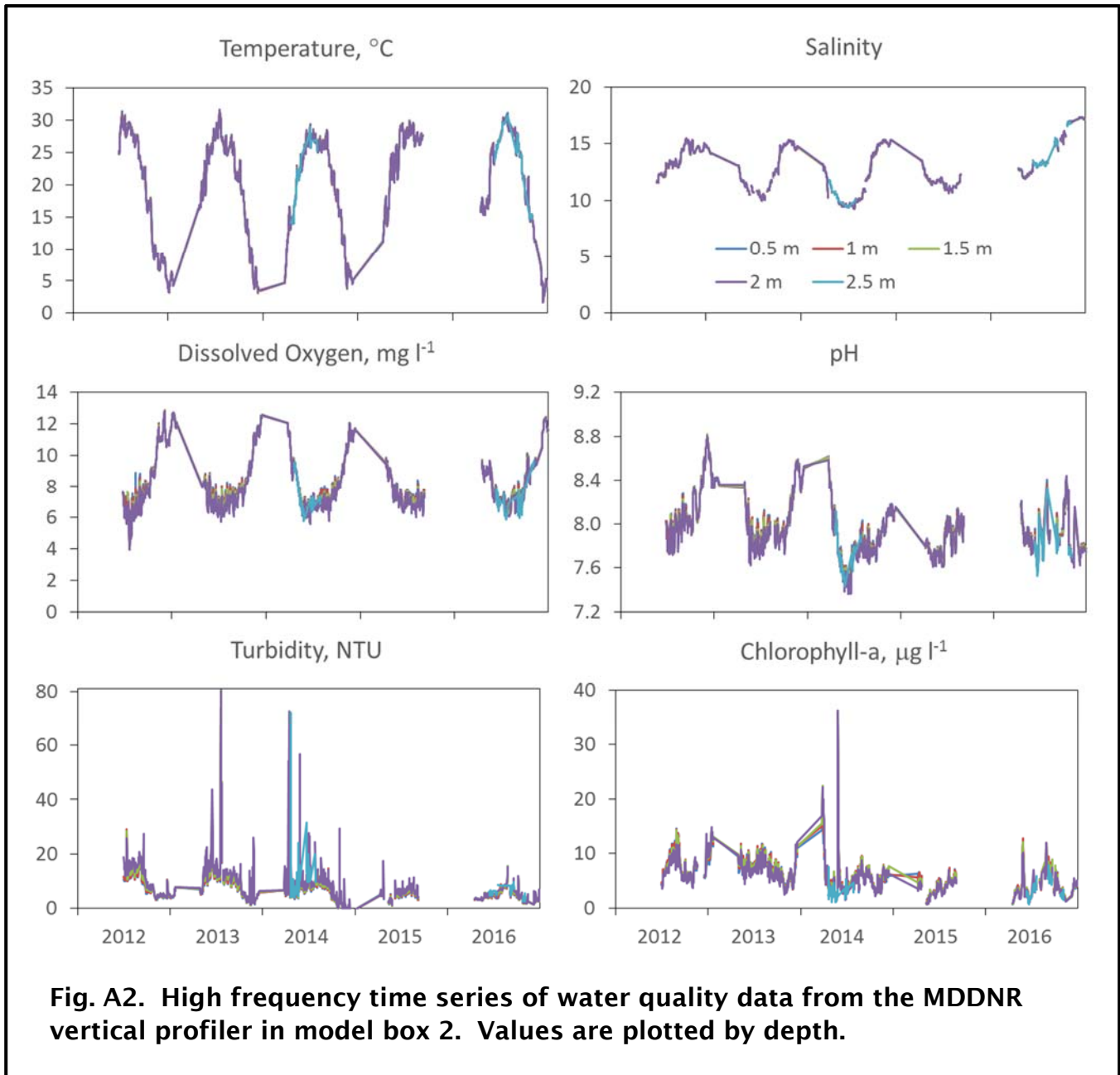


Fig. A2. High frequency time series of water quality data from the MDDNR vertical profiler in model box 2. Values are plotted by depth.

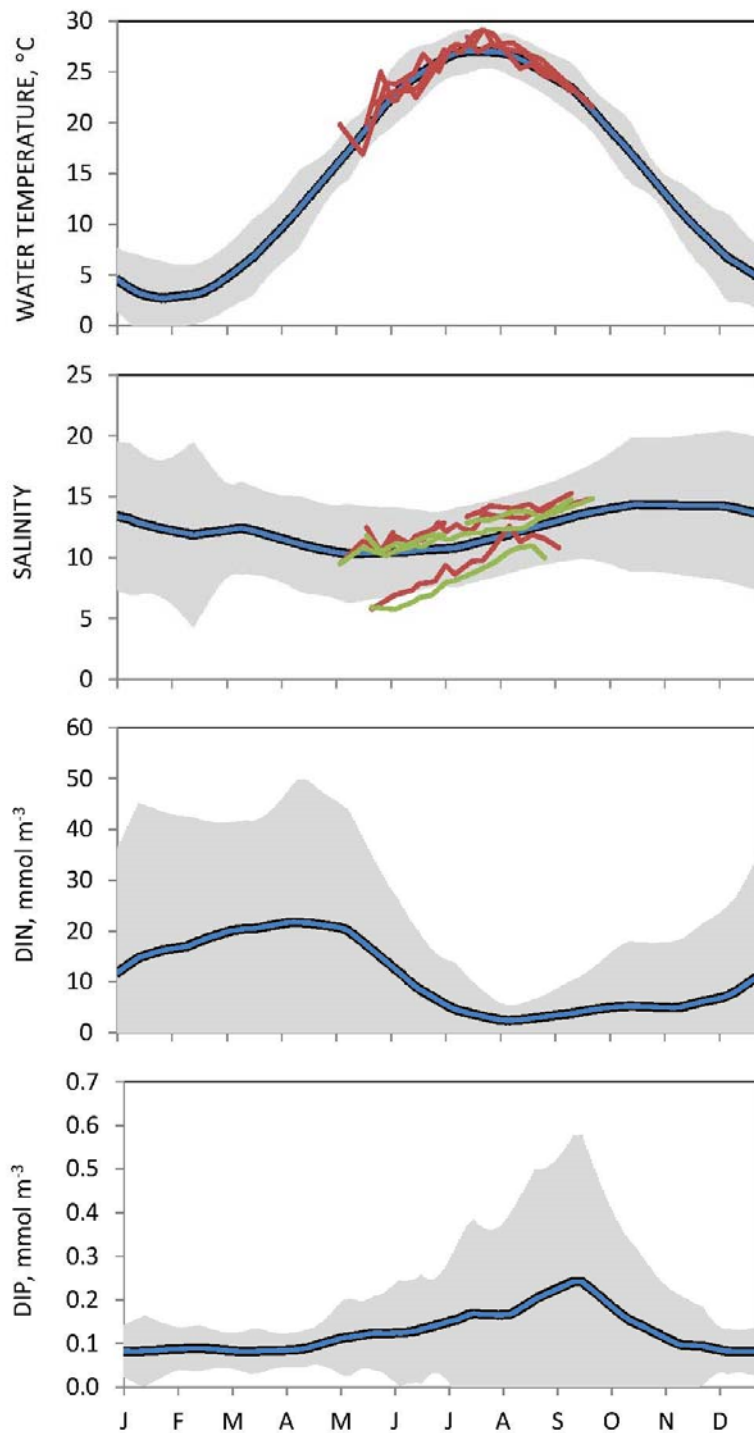


Fig. A3. Model boundary conditions. Blue line and shaded region depict the long-term (2000-16) average annual cycles \pm 2 s.d. from CBP station EE2.1. Red (station 2) and green (station 3) lines are UMCES data from all years at stations outside the model domain.

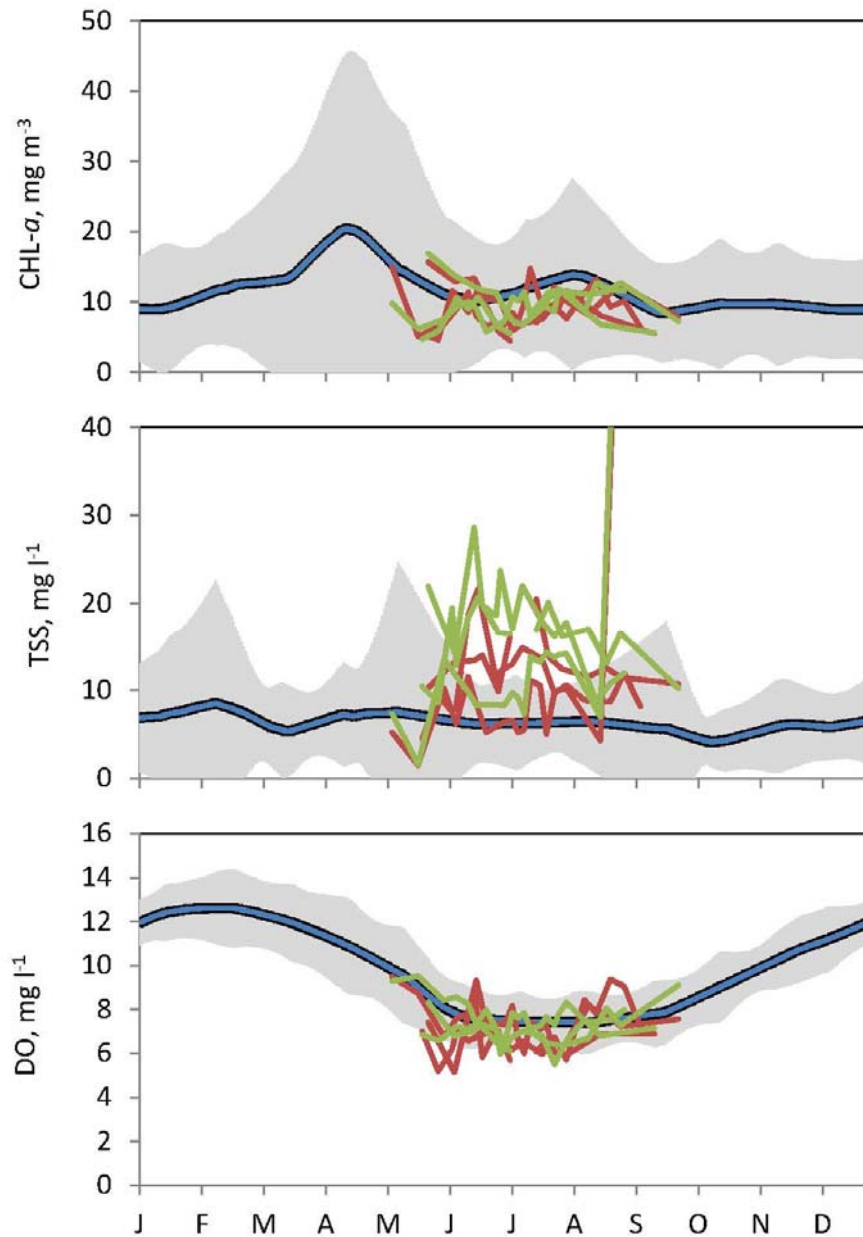


Fig. A4. Model boundary conditions. Blue line and shaded region depict the long-term (2000-16) average annual cycles \pm 2 s.d. from CBP station EE2.1. Red (station 2) and green (station 3) lines are UMCES data from all years at stations outside the model domain.

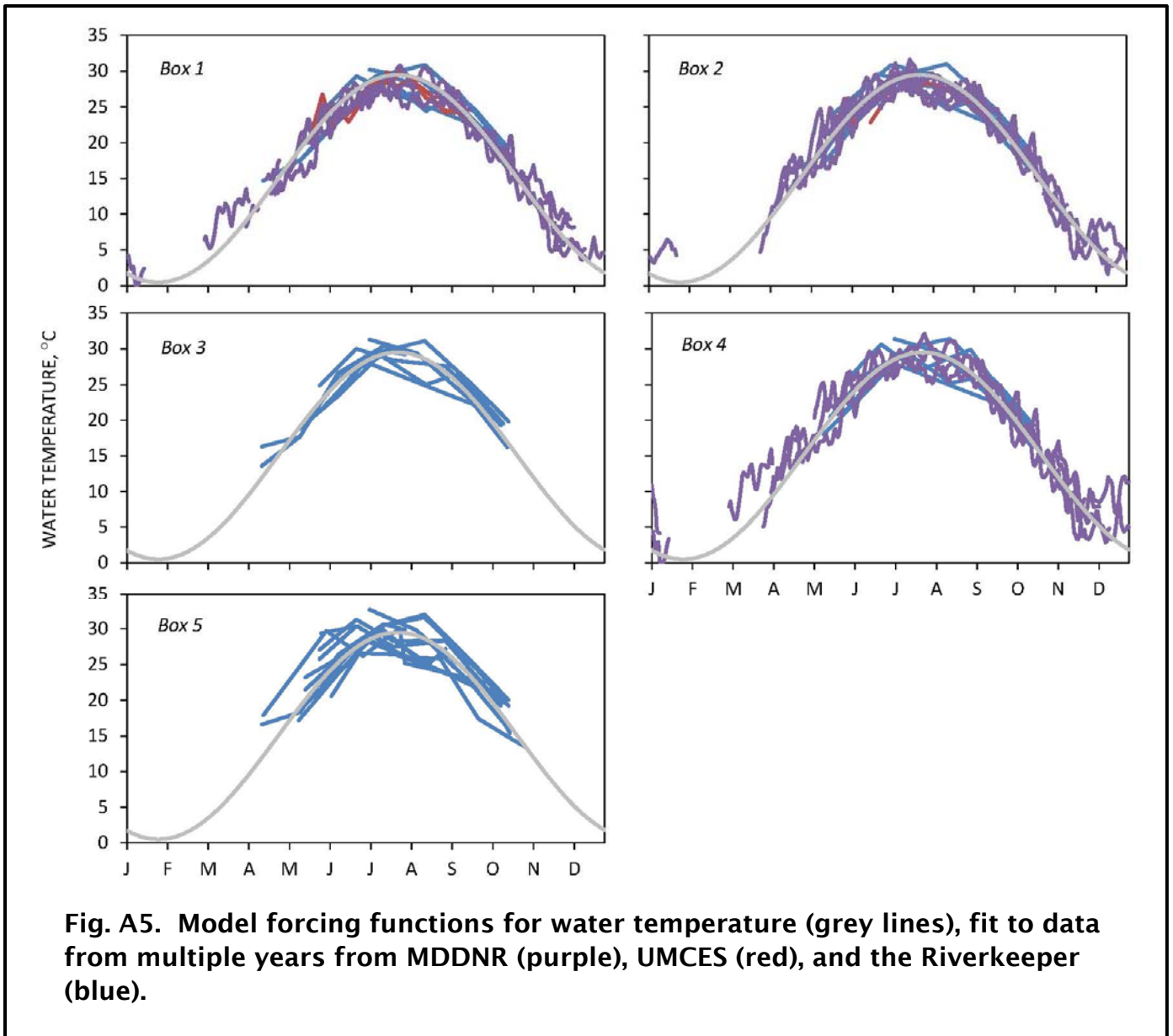


Fig. A5. Model forcing functions for water temperature (grey lines), fit to data from multiple years from MDDNR (purple), UMCES (red), and the Riverkeeper (blue).

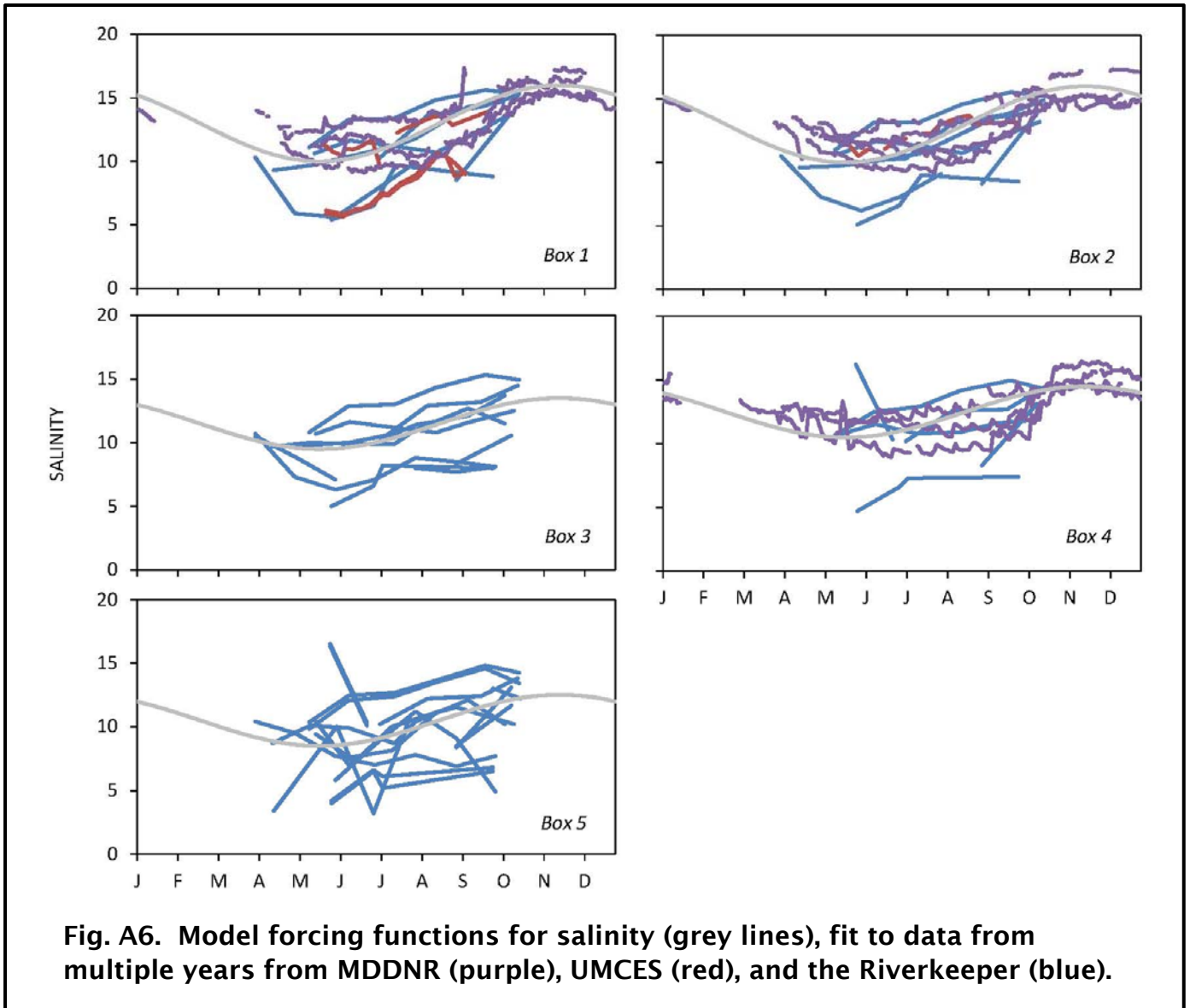


Fig. A6. Model forcing functions for salinity (grey lines), fit to data from multiple years from MDDNR (purple), UMCES (red), and the Riverkeeper (blue).

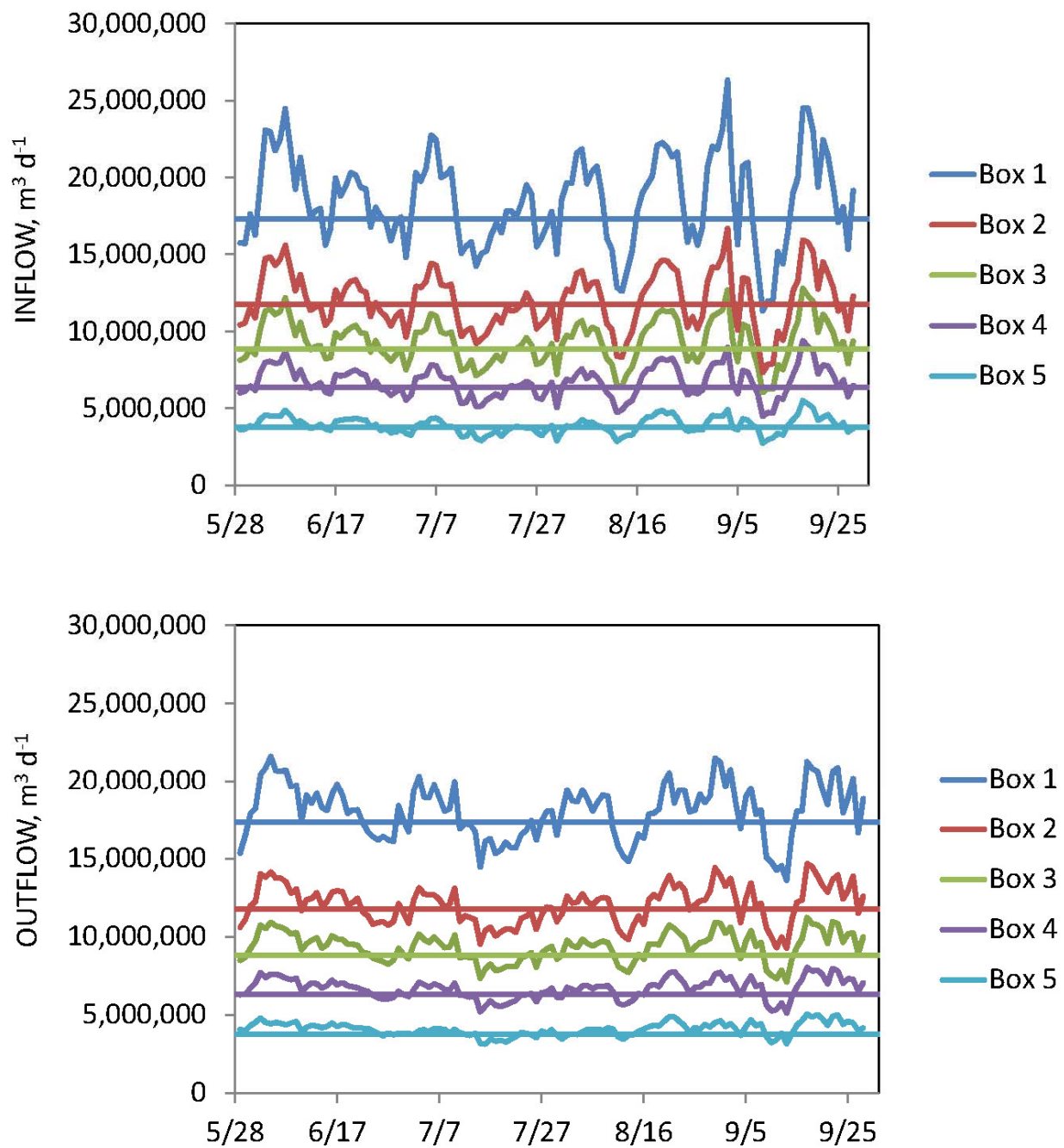


Fig. A7. Computed volume flows across the downstream boundary of each spatial element during flood tide (inflow, upper) and ebb tide (outflow, lower) using the tidal prism approach of the Harris Creek Model (straight lines), compared to flows computed by ChopROMS provided by Y. Lee and E. North, UMCES (lines with variability). See Kellogg et al. (2014) for more details.

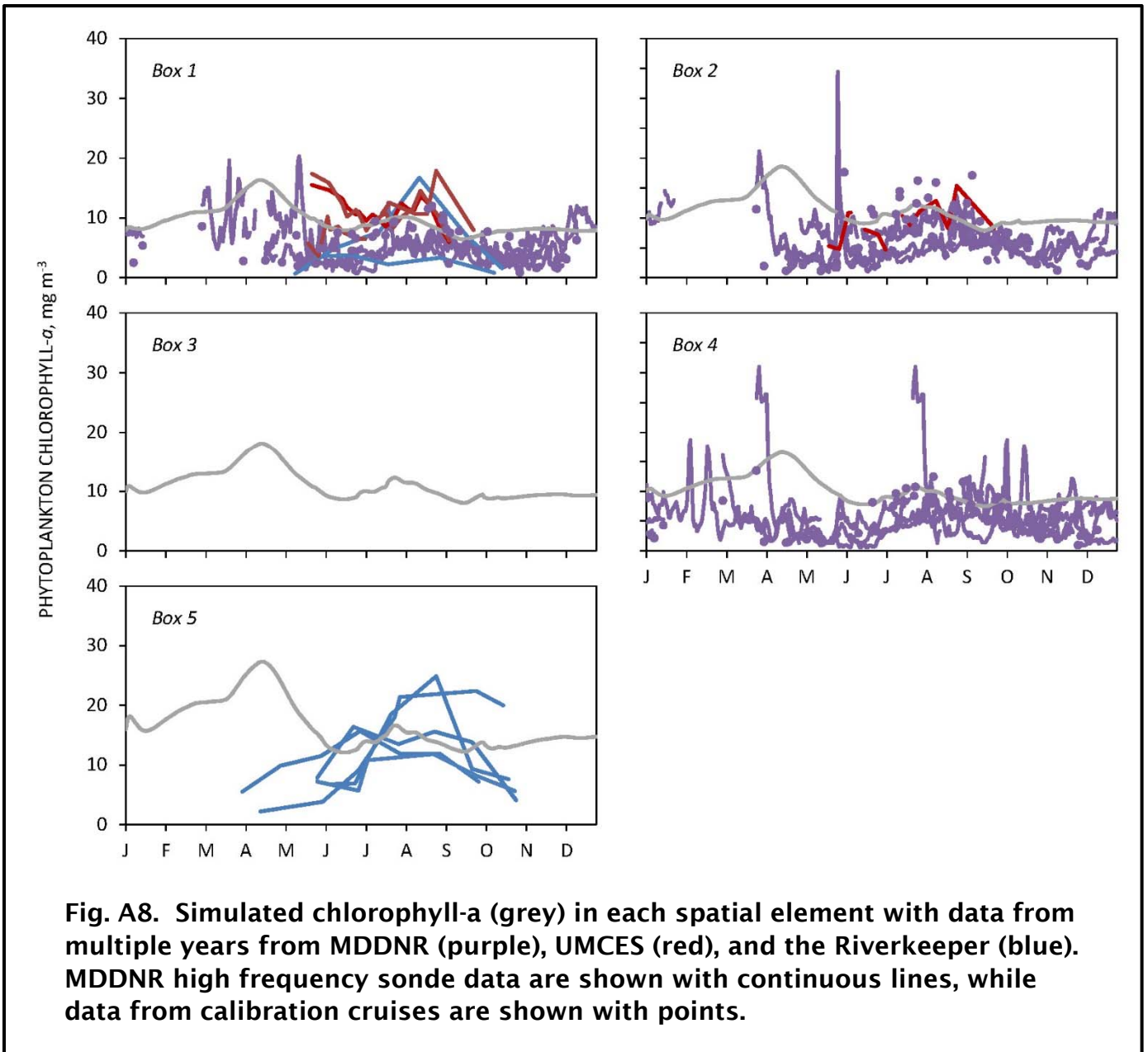


Fig. A8. Simulated chlorophyll-a (grey) in each spatial element with data from multiple years from MDDNR (purple), UMCES (red), and the Riverkeeper (blue). MDDNR high frequency sonde data are shown with continuous lines, while data from calibration cruises are shown with points.

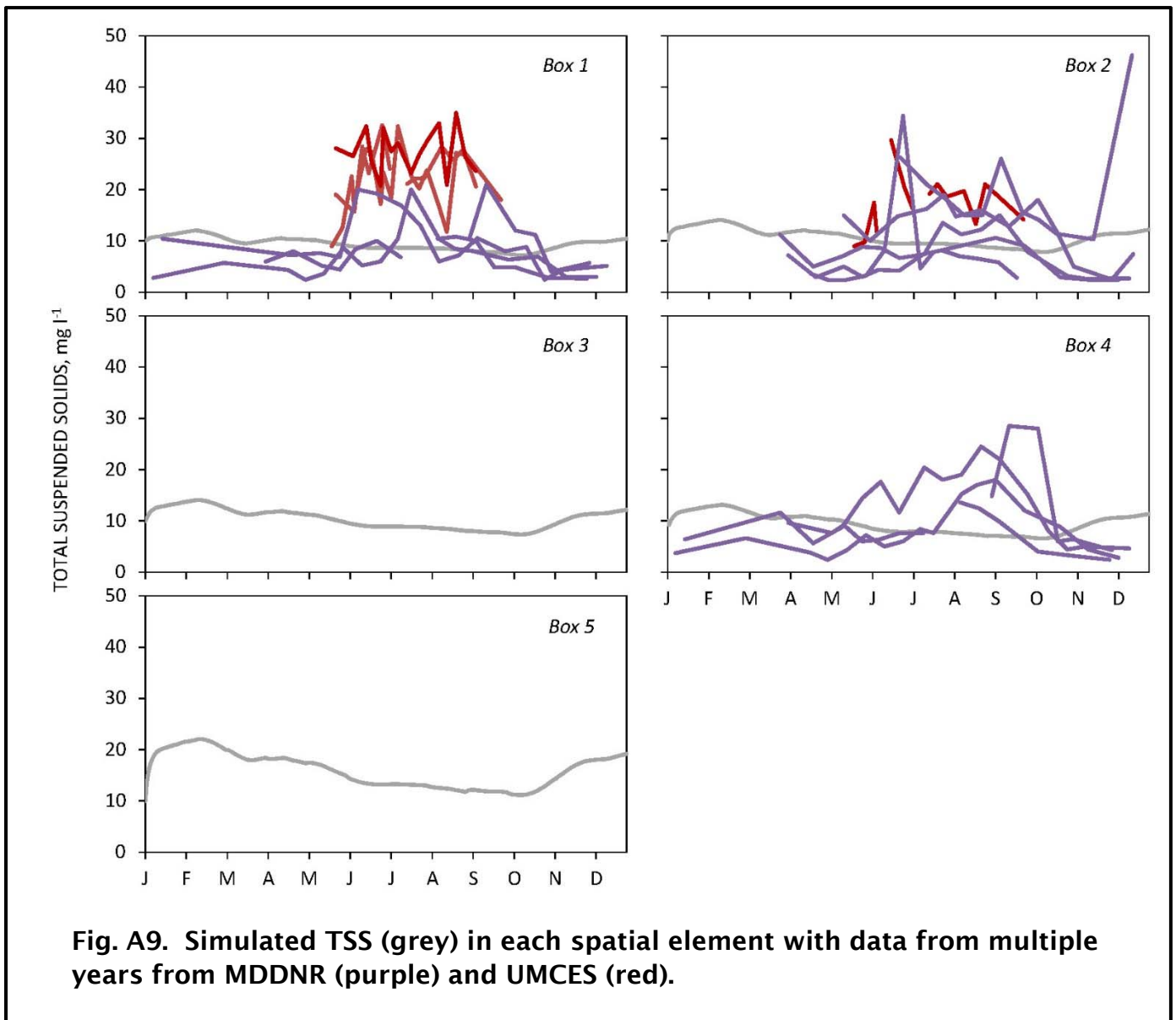


Fig. A9. Simulated TSS (grey) in each spatial element with data from multiple years from MDDNR (purple) and UMCES (red).

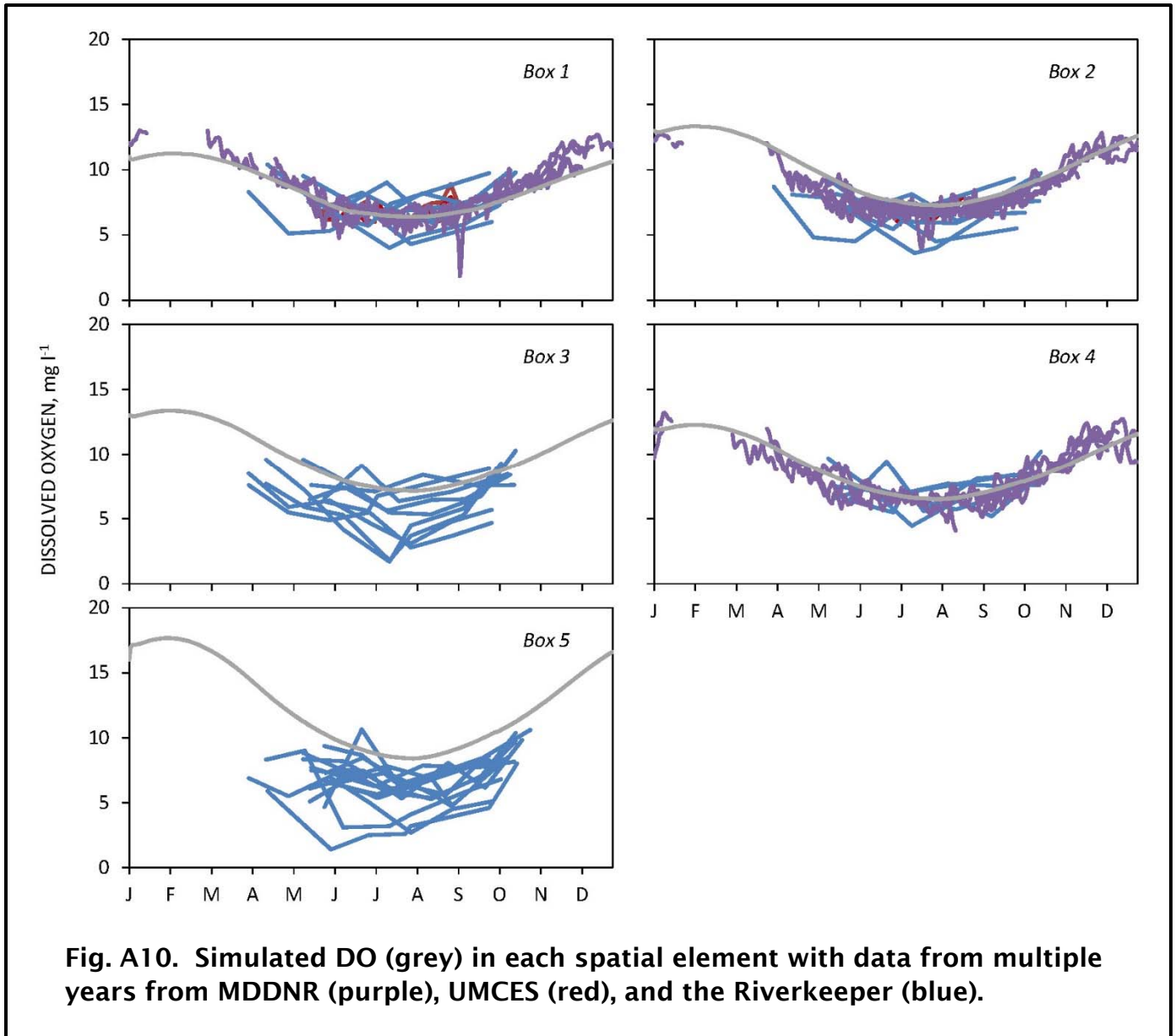


Fig. A10. Simulated DO (grey) in each spatial element with data from multiple years from MDDNR (purple), UMCES (red), and the Riverkeeper (blue).

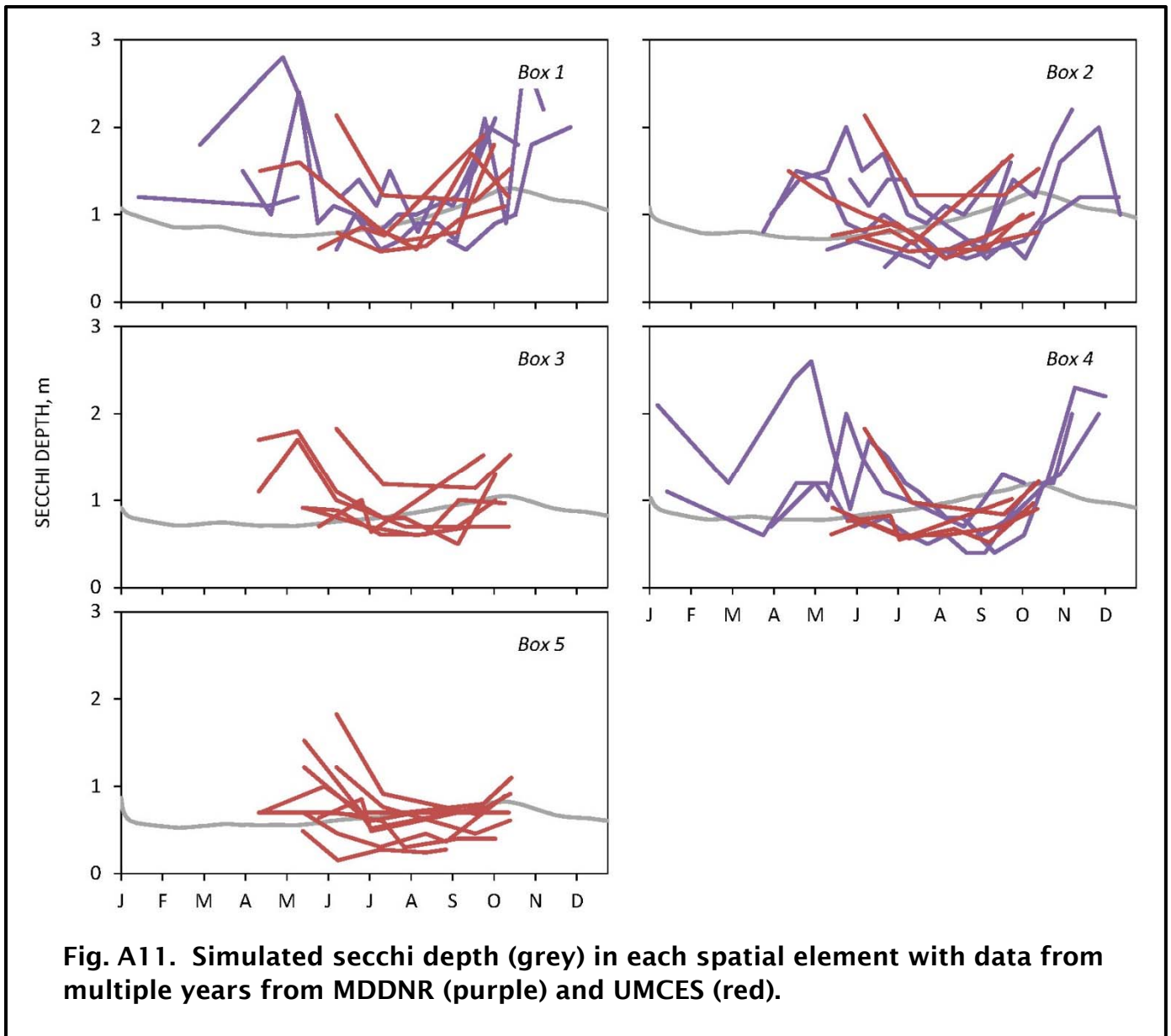
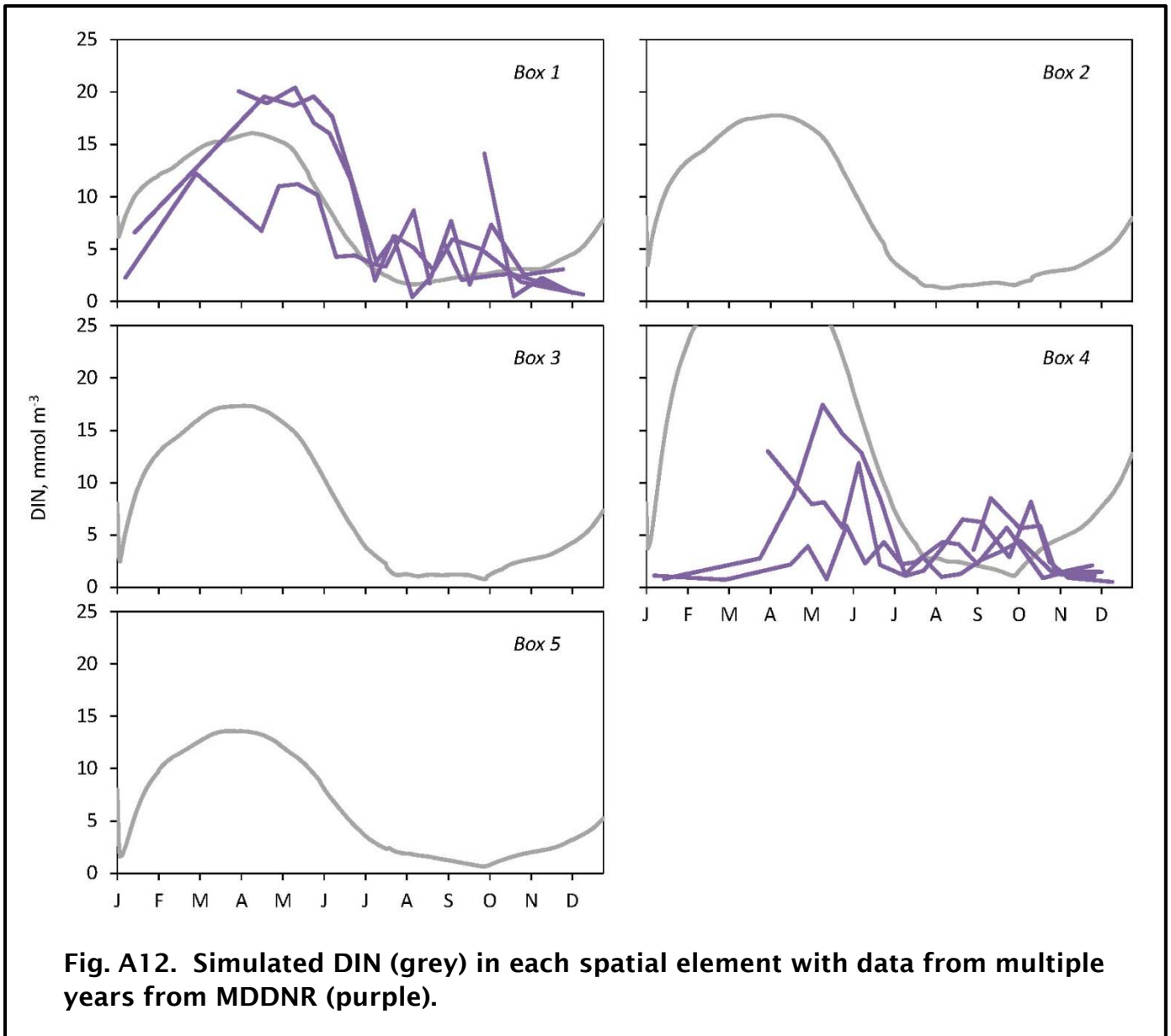


Fig. A11. Simulated secchi depth (grey) in each spatial element with data from multiple years from MDDNR (purple) and UMCES (red).



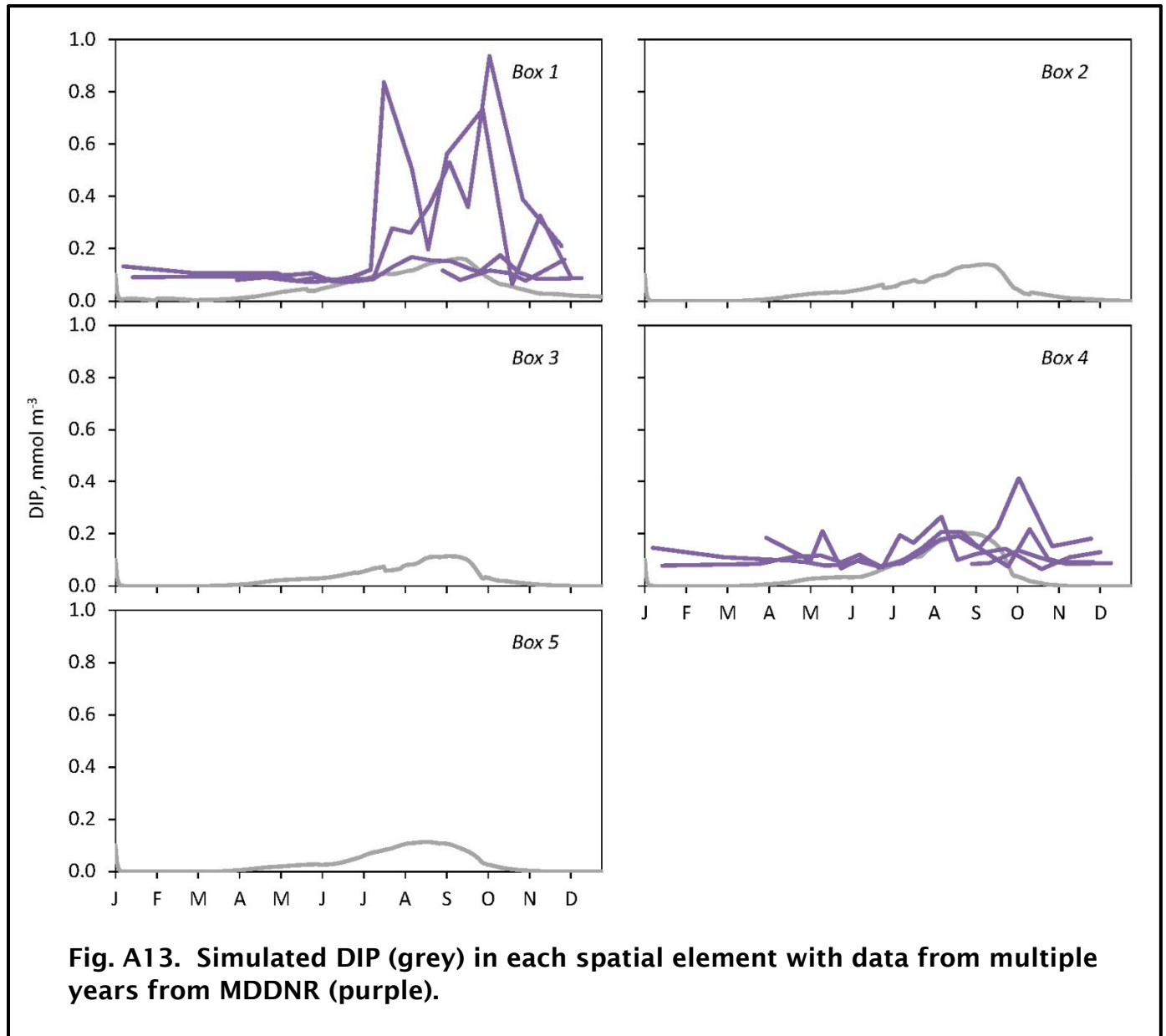


Fig. A13. Simulated DIP (grey) in each spatial element with data from multiple years from MDDNR (purple).

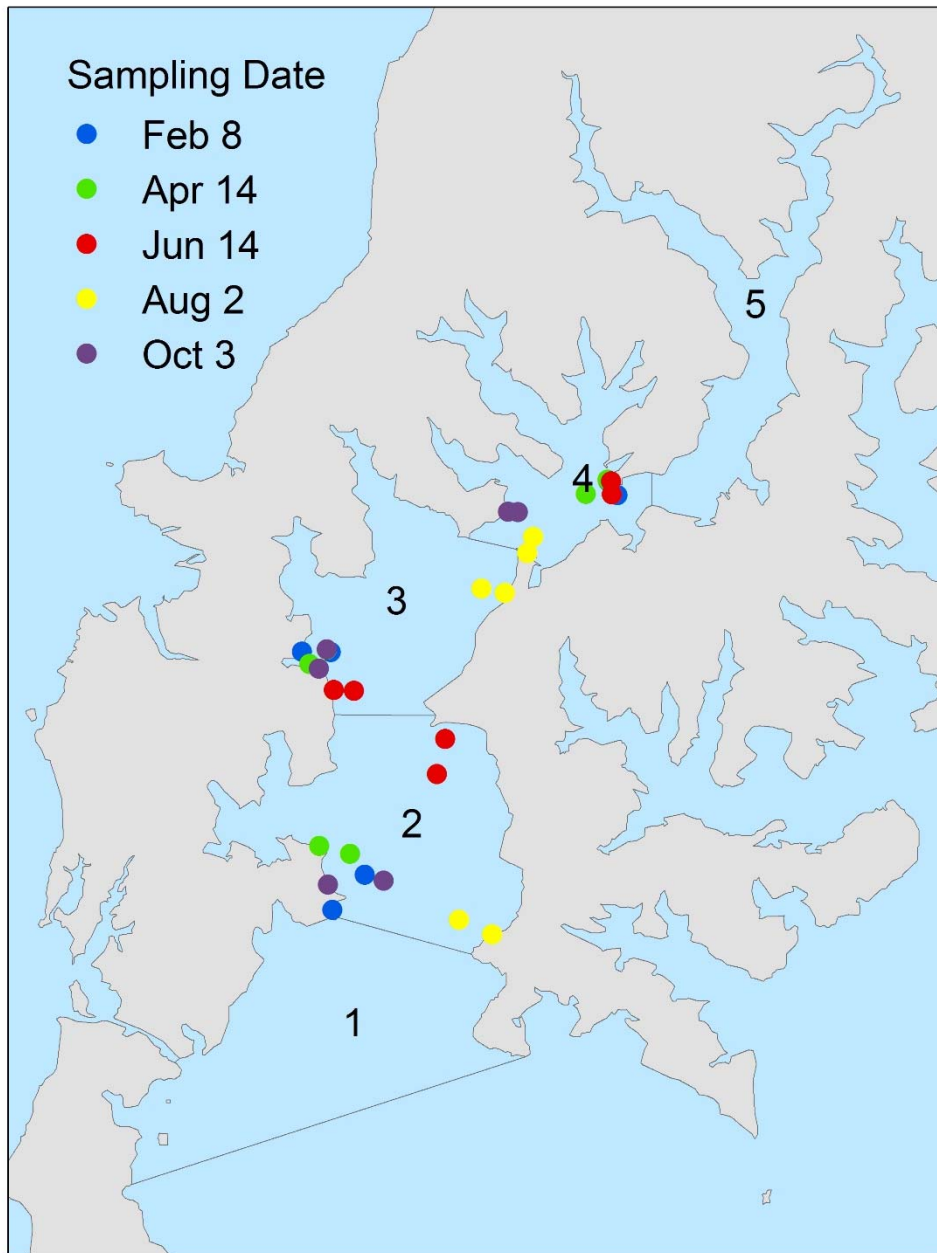


Fig. A14. Location of stations for 2016 BMA chl-a sampling. All data were collected in model boxes 2, 3, and 4. Each month, a random shoreline location was selected in each box, and BMA chl-a was sampled at 0.25, 0.75, 1.25, 1.75, 2.25, and 2.75 m. Map denotes the locations of the end-member samples on each date (i.e.. 0.25 and 2.75 m).

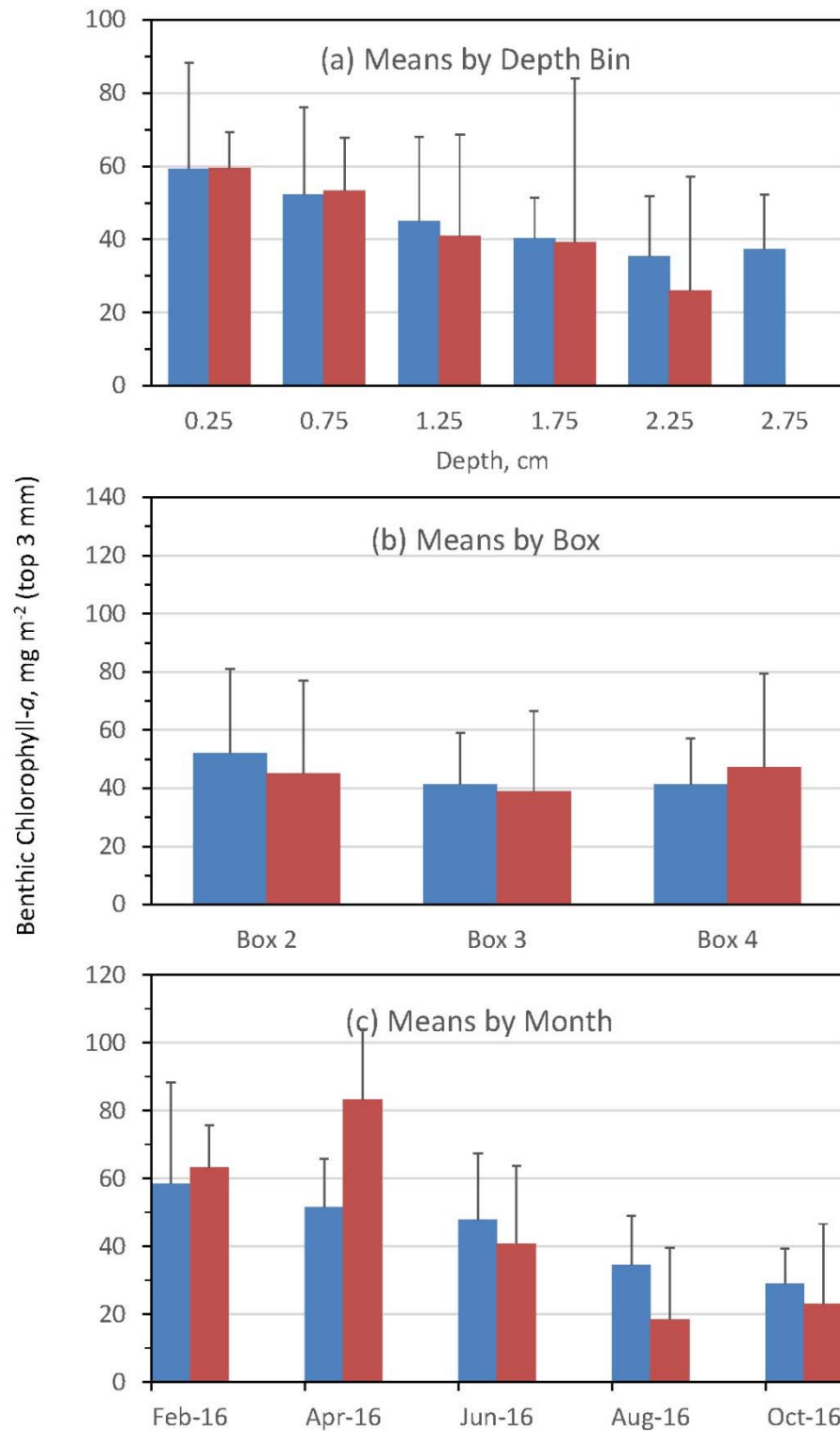


Fig. A15. Simulated BMA chl-a (red) compared to observed values from 2016 sampling (blue). Values are presented as means by (a) depth bin, (b) box, and (c) month. Error bars denote one standard deviation.

Appendix B: Online Model

Screen shots of the online model available at:

<https://exchange.iseesystems.com/public/markbrush/harris-creek-model-v2>

The Harris Creek Oyster Restoration Model v.2


Drs. Mark J. Brush and M. Lisa Kellogg
Virginia Institute of Marine Science
June 2018

[Introduction](#)


The Harris Creek model simulates water quality, ecosystem dynamics, and function of restored oyster reefs in five well-mixed boxes (Fig. 1). A diagram of the model is given on the next page (Fig. 2).

The model runs over an average annual cycle based on forced water temperature, salinity, and boundary conditions using Chesapeake Bay Program (CBP) data for 2000-16, additional water quality data for 2010-16 from the Maryland Department of Natural Resources, University of Maryland Center for Environmental Science, and Midshore Riverkeeper Conservancy, and monthly watershed loading from the CBP Phase V watershed model for 1985-2005.

The user can conduct runs under various restoration scenarios and export output on the following pages. The first version of the model (v.1, 2014) was funded by the National Fish and Wildlife Foundation and Oyster Recovery Partnership, while revisions to generate v.2 were funded by The Nature Conservancy, Chesapeake Bay Program.



Contact: Dr. Mark J. Brush
VIMS, PO Box 1346
Gloucester Point, VA 23062
804-684-7402; brush@vims.edu



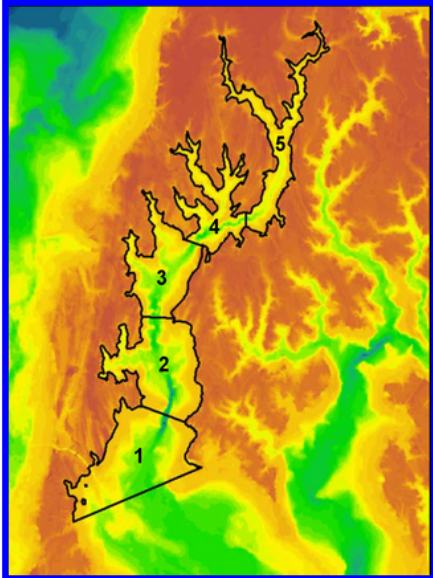


Fig. 1: Spatial elements (1-5) of the Harris Creek model.

Skip to Scenario Analysis

Next Page

Fig. B1. Opening page of the online model, with a brief introduction and contact information. A blue button for “Next Page” in the lower right corner allows the user to navigate through the site. The red button allows the user to skip directly to the scenario analysis page.

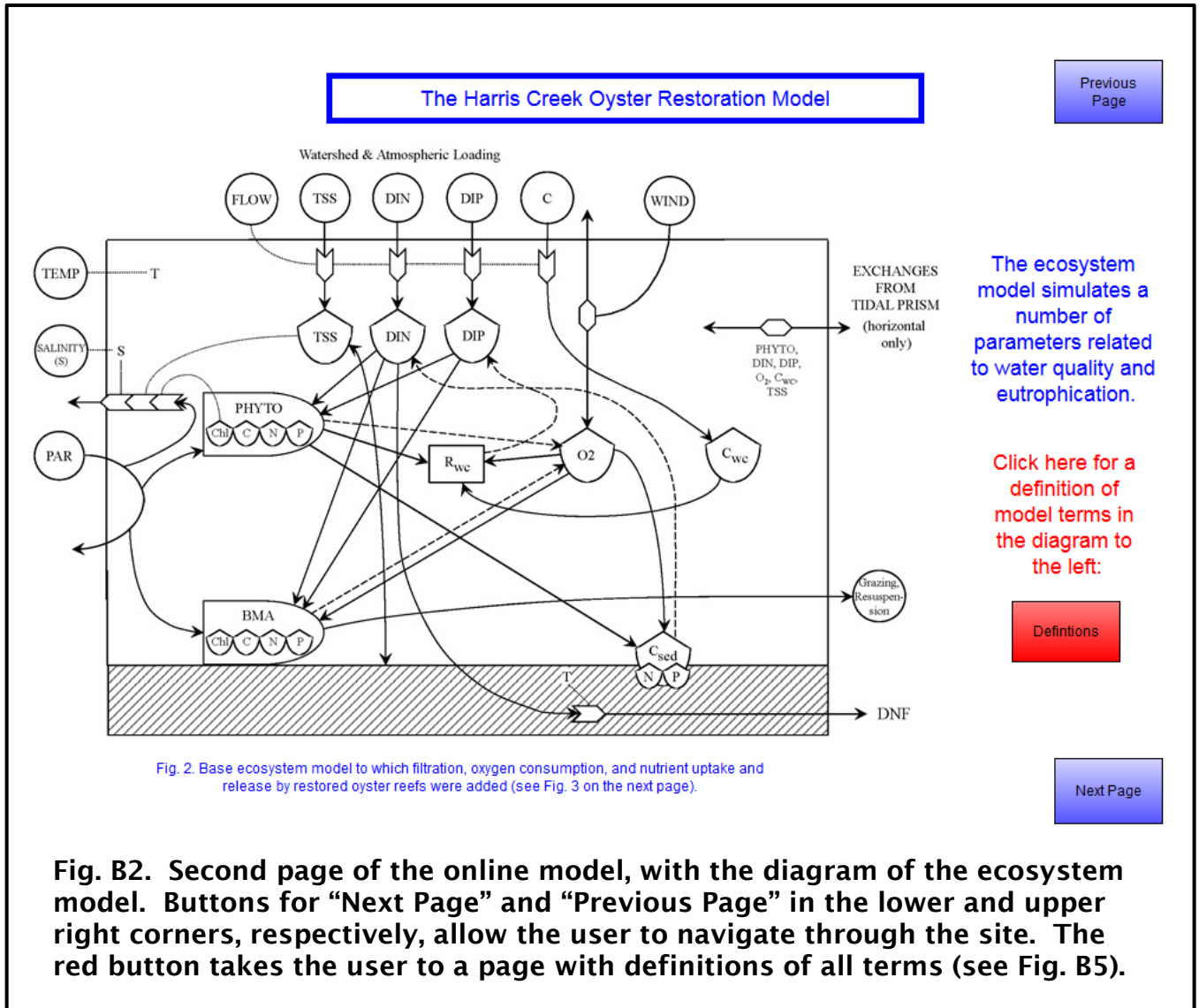


Fig. B2. Second page of the online model, with the diagram of the ecosystem model. Buttons for “Next Page” and “Previous Page” in the lower and upper right corners, respectively, allow the user to navigate through the site. The red button takes the user to a page with definitions of all terms (see Fig. B5).

The Harris Creek Oyster Restoration Model

Previous Page

The diagram illustrates the oyster submodel's nutrient dynamics. At the top left, a box labeled 'PHYTO' contains 'Chl', 'C', 'N', and 'P'. A blue arrow labeled 'Ingestion (I_{oy})' points from PHYTO to a central box for *C. virginica*. Above this box is a 'TSS' box. To the right, 'Assimilated Nutrients (A_{oy})' is defined as $A_{oy} = I_{oy} - R_{oy} - F_{oy}$. Below this, 'DIN' and 'DIP' boxes are shown. A red arrow labeled 'Respiration & Recycle (R_{oy})' points from *C. virginica* to a box containing 'O₂'. Below the oyster box, 'N_{shell}', 'P_{shell}', 'N_{tissue}', and 'P_{tissue}' are listed. An arrow points from the oyster box to a box labeled 'Burial (B_{oy})'. Below that, 'Feces & Pseudofeces (F_{oy})' is shown, with an arrow pointing to 'DNF_{oy}'.

The oyster sub-model simulates a number of parameters related to the impact of oyster restoration.

Click here for a definition of model terms in the diagram to the left:

Definitions

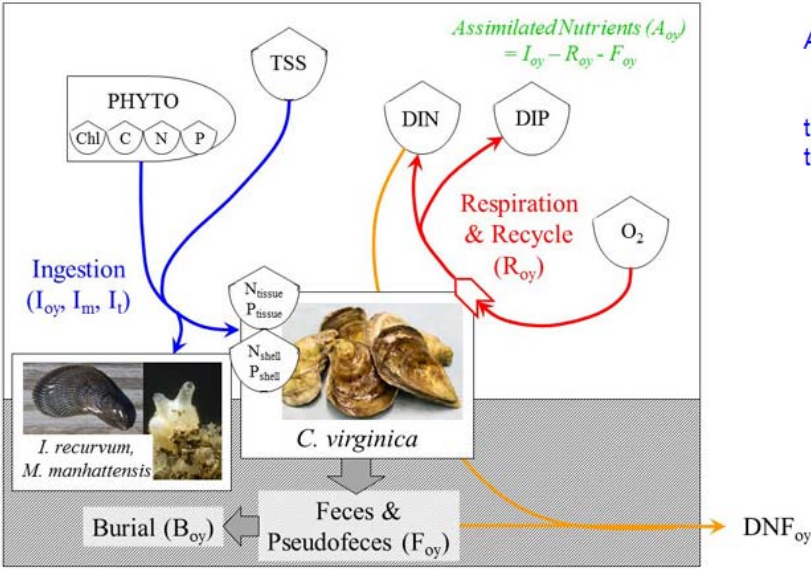
Fig. 3. Oyster submodel with linkages to the base ecosystem model in Fig. 2.
Photo: New York State Department of Environmental Conservation.

Next Page

Fig. B3. Third page of the online model, with the diagram of the oyster sub-model. Buttons for “Next Page” and “Previous Page” in the lower and upper right corners, respectively, allow the user to navigate through the site. The red button takes the user to a page with definitions of all terms (see Fig. B5).

The Harris Creek Oyster Restoration Model

Previous Page



Additional filtration by reef-associated mussels and tunicates were added to the revised version of the model.

Click here for a definition of model terms in the diagram to the left:

Definitions

Fig. 4. Oyster submodel with addition of mussel and tunicate filtration.

Mussel photo: B. Hubick, Maryland Biodiversity Project;
Tunicate photo: M. Decler, World Register of Marine Species.

Next Page

Fig. B4. Fourth and new page of the online model, showing the addition of mussel and tunicate filtration to the oyster sub-model.

Model Definitions Page

Ecosystem model definitions:

Properties around the perimeter of the box are forced; properties within the box are simulated.

BMA = benthic microalgal biomass

C = carbon
Chl = chlorophyll-a
Csed = sediment organic C

Cwc = water column C

DIN = dissolved inorganic N

DIP = dissolved inorganic P
FLOW = daily freshwater inflow

N = nitrogen
O2 = dissolved oxygen
P = phosphorus
PAR = photosynthetically active radiation

PHYTO = phytoplankton biomass

Dwc = water column respiration

Oyster submodel definitions:

Aoy = oyster assimilation

Boy = oyster-mediated burial

DNFoy = oyster-mediated denitrification

Foy = oyster production of feces and pseudofeces

loy = oyster ingestion
lm = mussel ingestion
lt = tunicate ingestion

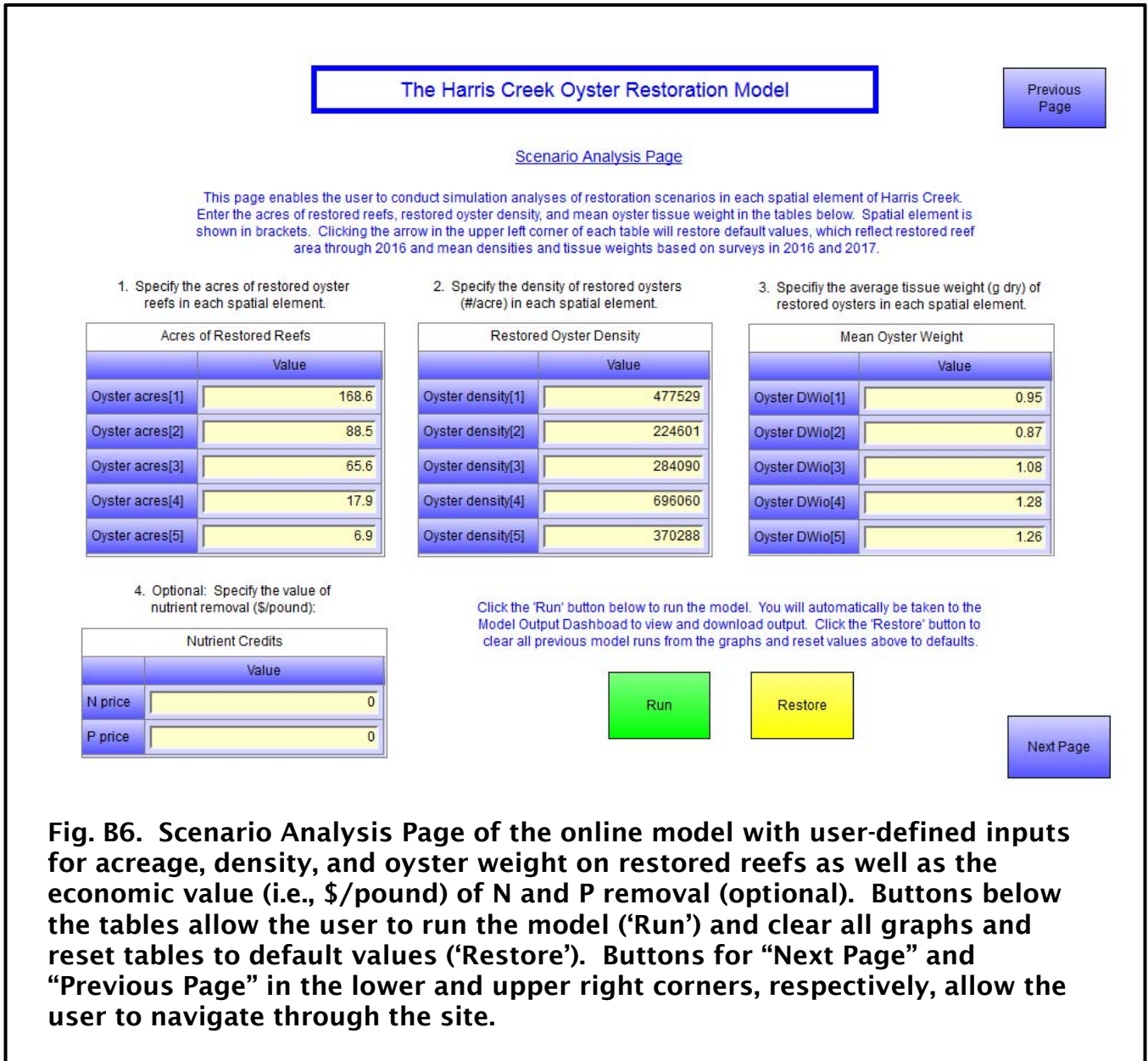
Nshell = N contained in oyster shell
Ntissue = N contained in oyster tissue

Pshell = P contained in oyster shell
Ptissue = P contained in oyster tissue

Roy = oyster respiration and nutrient recycle

[Back to Ecosystem Model diagram](#) [Back to Oyster Sub-Model diagram](#)

Fig. B5. Fifth page of the online model, with definitions of terms found in the model diagrams on Pages 2-4. Buttons return the user to either Page 2 (ecosystem model diagram) or Page 3 (oyster sub-model diagram).



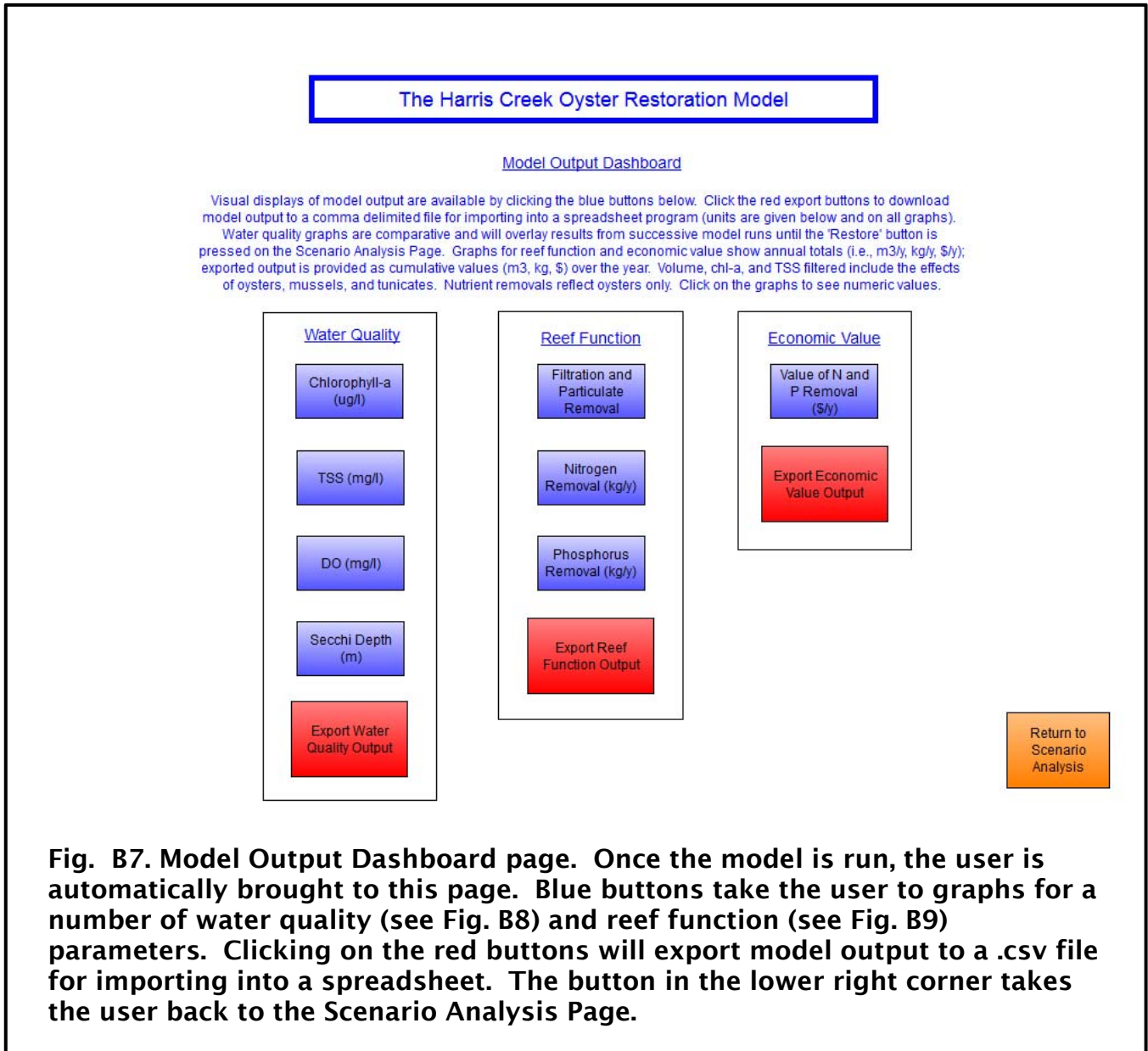


Fig. B7. Model Output Dashboard page. Once the model is run, the user is automatically brought to this page. Blue buttons take the user to graphs for a number of water quality (see Fig. B8) and reef function (see Fig. B9) parameters. Clicking on the red buttons will export model output to a .csv file for importing into a spreadsheet. The button in the lower right corner takes the user back to the Scenario Analysis Page.

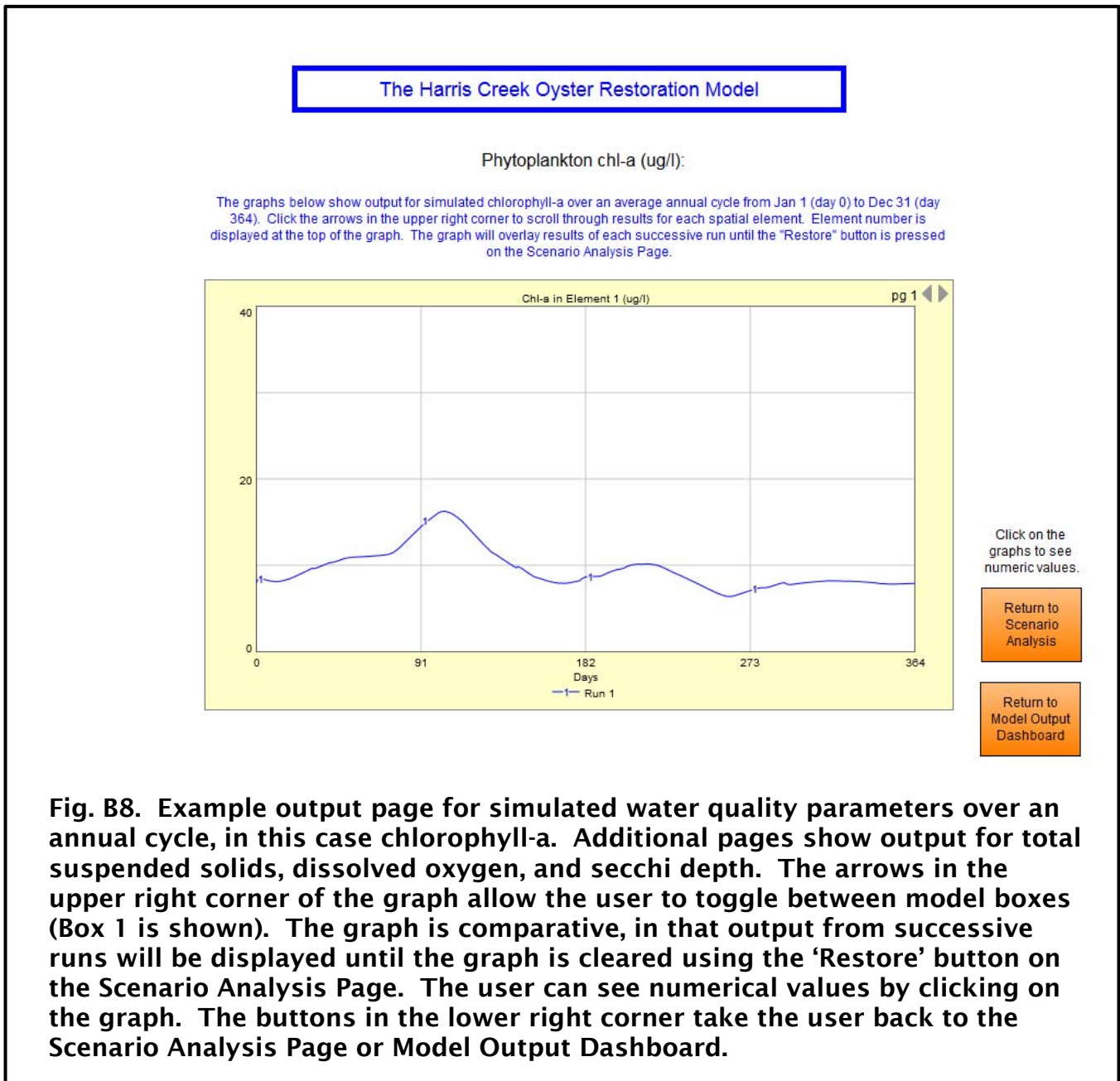


Fig. B8. Example output page for simulated water quality parameters over an annual cycle, in this case chlorophyll-a. Additional pages show output for total suspended solids, dissolved oxygen, and secchi depth. The arrows in the upper right corner of the graph allow the user to toggle between model boxes (Box 1 is shown). The graph is comparative, in that output from successive runs will be displayed until the graph is cleared using the 'Restore' button on the Scenario Analysis Page. The user can see numerical values by clicking on the graph. The buttons in the lower right corner take the user back to the Scenario Analysis Page or Model Output Dashboard.

